The Hoyle state in 12C

Freer, Martin; Fynbo, H.o.u.

Accepted Manuscript

The Hoyle state in ^{12}C
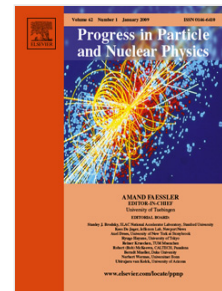
M. Freer, H.O.U. Fynbo

The Hoyle state in ^{12}C

M. Freer,[1] H.O.U. Fynbo[2]

[1]School of Physics and Astronomy, University of Birmingham,
Birmingham, B15 2TT, United Kingdom
[2]Department of Physics and Astronomy, Aarhus University,
DK-8000 Aarhus C, Denmark

June 6, 2014

Abstract

The 7.65 MeV, $J^\pi=0^+$, second excited state in ^{12}C is known as the Hoyle-state after Fred Hoyle. In the 1950s Hoyle proposed the existence of the state in order to account for the stellar abundance of carbon. Aside from its key role in the synthesis of the elements it is believed to possess a rather unusual structure, where the dominant degrees of freedom are those of α-particle clusters rather than nucleons. An understanding of the properties of the Hoyle state, for example its radius and excitations, has been the focus of a major experimental activity. Similarly, unravelling precisely why a cluster state should arise at precisely the right energy to promote synthesis of carbon has been a central theoretical challenge. To a significant extent, the Hoyle-state has become a cornerstone for state-of-the-art nuclear theory. This review examines the present status of both theory and experiment and indicates directions for future developments to resolve some of the remaining open questions.

1

Contents

1 Introduction

There are few nuclei that have captured the imagination more than carbon-12. Its' synthesis is key to the origins of organic life and has fueled the rapid economic development of mankind since the industrial revolution. The gateway through which that synthesis proceeds is dominated by the presence of the second excited state at 7.65 MeV, $J^\pi = 0^+$ in ^{12}C; the Hoyle-state.

The synthesis of carbon-12 in the helium burning phase proceeds through what is known as the triple α-process [1, 2], where first two α-particles fuse to form ^{8}Be whose instability to α-decay results in an equilibrium concentration of ^{8}Be. The second step is the capture by ^{8}Be to form ^{12}C at an excitation close to 7.5 MeV followed by electromagnetic decay to the ^{12}C ground state. Hoyle recognised the need for a $J^\pi = 0^+$ state close to this energy in order to account for the absolute abundance of ^{12}C and the relative abundance of ^{12}C and ^{16}O [3]. The capture of the α-particle by ^{8}Be proceeds by tunneling through the mutual barrier. This barrier has two components; the Coulomb and centrifugal barrier. For s-wave capture the centrifugal barrier vanishes, and the probability of carbon-12 formation is maximised. The presence of the Hoyle-state at 7.65 MeV resonantly boosts the capture process by a factor of close to 10-100 million. Hoyle predicted the existence of a state at 7.68 MeV [3], and whilst a visitor at Kellogg Laboratory at Caltech, convinced the local group to search for the state. They measured the ^{14}N(d,α)^{12}C reaction using a high resolution spectrometer at which point a state at 7.68 MeV was observed [4]. Subsequent measurements refined the energy of the state to 7.653±0.008 MeV and indicated the most probable spin and parity to be 0^+ [5].

The connection between the existence of organic life and ultimately human-kind has led to the interpretation [6] that the prediction of the existence of 7.65 MeV state by Hoyle was an outstanding

example of the anthropic principle, an idea introduced by Carter in 1973 [7]. The principle relies on the fact that intelligent life exists, to assert certain properties of the universe must exist, i.e. we exist therefore so must the 7.65 MeV state in ^{12}C. The question as to if Hoyle deployed the anthropic principle or not has been the subject of some debate, recently reviewed by Kragh [8]. The strong conclusion was that Hoyle's reliance was on the challenge of understanding the natural abundance of ^{12}C and ^{16}O (the latter produced by capture of an α-particle on ^{12}C) that drove his prediction, rather than a deeper connection to his own existence. Indeed, it is apparent that there was experimental evidence for the existence of the Hoyle-state which predated the measurements of the Caltech group [4]. A measurement of the ^{14}N(d,α)^{12}C reaction by the Cornell group [9] published in 1940 indicated the existence of a state at 7.62 MeV, though subsequent measurements had failed to confirm its existence [10]. Crucially, it would appear Hoyle was not aware of these earlier measurements when making his prediction [8].

The existence of the state at the right energy (within a few hundred keV) with the right properties, even if its existence was not predicted anthropically, is truly remarkable. This may be a happy accident of nature, or perhaps there is a deeper significance. For example, it is possible that the state might possess a particular structure which would place it close to, and indeed above, the α-decay threshold in ^{12}C (7.367 MeV).

Even predating the above first experimental hint of the existence of the 7.65 MeV state in 1940 [9], Hafstad and Teller [11] (1938) analysed the binding energy behaviour of the ground states of $N = Z$, N even, nuclei (α-conjugate nuclei), e.g. ^{8}Be, ^{12}C, ^{16}O .... A linear dependence was found between the number of inter α-particle bonds (e.g. ^{8}Be - 1, ^{12}C - 3, ^{16}O - 6, ...) and the binding energies, indicating that there was a fixed energy associated with the α-α interaction and further that the α-clusters featured within the ground-states of these systems. This view of the ground-states fell from favour as the single-particle description of nuclei became vogue and, in fact, was indeed an over simplification of the structural properties. Some thirty years later Ikeda and co-workers proposed a threshold picture for the appearance of cluster states [12]. The essence is that close to decay thresholds it is possible for nuclei to undergo structural changes. For example, the ground state of ^{8}Be being unbound to decay to two α-particles by 92 keV, might have a well-developed α-cluster structure. The ^{8}Be+α decay threshold, or equivalently 3α decay threshold (7.274 MeV), would permit the internal excitation energy to be transformed into the binding energy of the clusters as displayed in the Ikeda diagram shown in Fig. 1 [12].

This opens up the possibility that close to the region occupied by the Hoyle-state that there exists the optimal conditions for the transformation of the ^{12}C nucleus into a sub-structure of three α-particles. In other words, the reason that Hoyle-state might exist at an energy just above the α-decay threshold could be associated with the fact that it possesses a 3α-cluster structure. In turn it is the link between clustering and thresholds which is the remarkable coincidence which lies behind the origins of the abundance of carbon-12.

The fact that nuclei have the facility to cluster is a deeper question which necessitates that the subunits, in this case α-particles, should have greater stability of the composite system, taking into account the internal energy. The fact that the ^{4}He nucleus possesses a significantly higher binding energy per nucleon than its neighbours and a very high-lying first excited state (20.2 MeV, 0^{+}) makes it both a rather robust and inert sub-unit. These properties of the α-particle may be traced to the details of the strong interaction that fundamentally bind the nucleons in the nucleus.

The fact that the Hoyle-state plays a central role for nucleosynthesis and potentially has a cluster-type structure which links to the nature of strong interaction means that at every level there is a connection with the observed abundance of carbon-12. The Hoyle-state has thus become a touchstone for nuclear astrophysics, nuclear structure and nuclear forces. It is apparent that understanding the nature of this state could, in principle, simultaneously unlock many problems. The Hoyle-state has even been used to constrain the running light quark masses [13]. It is also possible that the bosonic nature of the α-particle could signal that the Hoyle-state is associated with nuclear matter in which
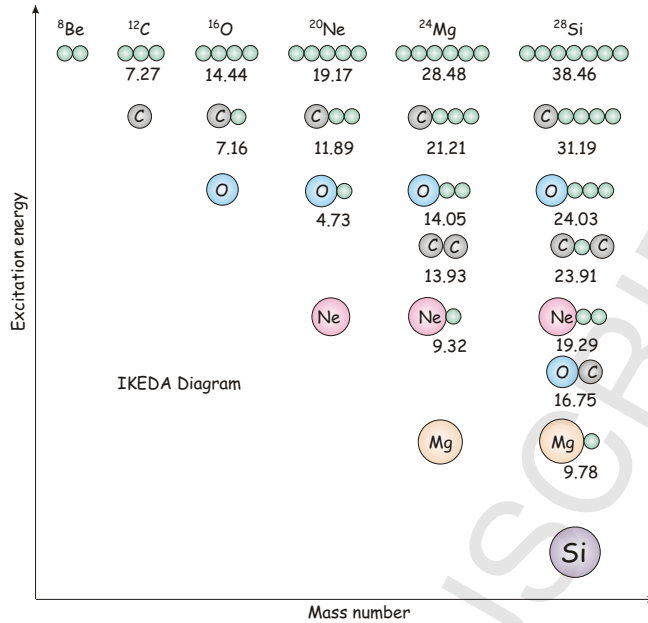
Figure 1: The Ikeda threshold diagram. This illustrates that for the ^{12}C nucleus above 7.27 MeV it is possible for the system to form into a structure of 3α-particles.

the important degrees of freedom are bosonic rather than fermionic - akin to an atomic Bose Einstein Condensation (BEC) [14].

This review examines the current understanding of the structure of the Hoyle-state and its connection with the most recent state-of-the-art nuclear models.

2 The Hoyle-state in nucleosynthesis

The *historical* development of the understanding of the synthesis of ^{12}C within stars has been substantially reviewed by Kragh [8], see also the detailed description by Rolfs and Rodney [15]. The work that was the forerunner to that of Hoyle came from Hans Bethe [16]. Bethe had concluded in 1939 that the formation of ^{12}C from the collision of three α-particles within stars was highly improbable, concluding that a temperature some 50 times higher than that known within stars such as the Sun was required [16]. The first significant step forward was provided by Öpik in 1951 who recognised that elevated temperatures were possible in stars in the red giant phase [1]. Salpeter in 1952 [2] then suggested that rather than the direct simultaneous capture of three particles a sequential process is preferred

$$^4\text{He} +^4\text{He} \rightarrow^8 \text{Be} \tag{1}$$

$$^8\text{Be} +^4\text{He} \rightarrow^{12} \text{C} + \gamma \tag{2}$$

The ^{8}Be nucleus was known to be unbound to 2α-decay, by an amount which is now known to be 92 keV, furthermore it has a width of 5.6 eV implying a lifetime of about 10^{-16} seconds. The energy of 92 keV is remarkably close to the peak of the Gamow window for α-burning temperatures close to 10^8 K (the peak of the Gamow window is approximately 85 keV with a width of 60 keV) [17]. The energy width of the ^{8}Be ground state is constrained by the Coulomb barrier, through which the α-decay (or

4
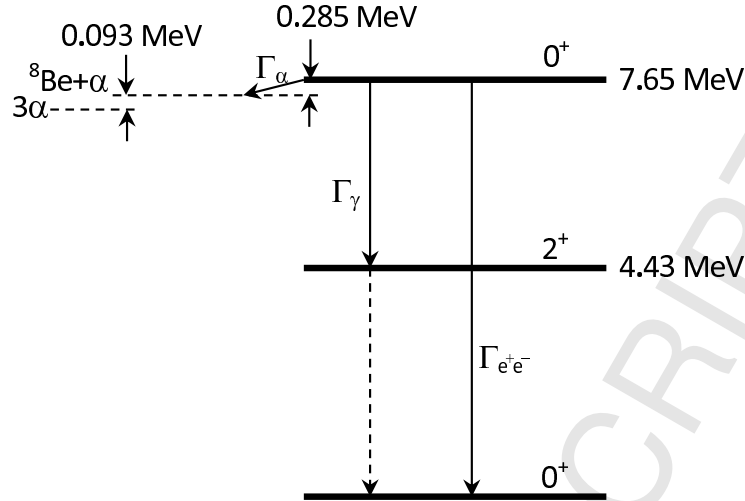
Figure 2: Schematic of the decay process by which ^{12}C is formed from the radiative ^{8}Be+^{4}He capture.

capture) must proceed. If the Q-value had been somewhat higher then the width would have been significantly larger, the lifetime shorter and the state would be located outside the Gamow window. These factors would dramatically affect the equilibrium abundance of ^{8}Be in a helium-seeded plasma. The stellar temperature of 2×10^8 K estimated by Salpeter and a density close to 100 g/cm^3 produces an equilibrium concentration ^{8}Be:^{4}He of 10^{-10}:1 [2]; clearly small, but significant.

The second step proceeds via the capture of a third α-particle before the ^{8}Be decays back into two α-particles. In this case the ^{4}He+^{8}Be$\rightleftharpoons^{12}$C* equilibrium is broken by the small leakage to the ^{12}C ground state facilitated by the radiative branches; either two gamma-decay, $0^+ \to 2^+ \to 0^+$, or e$^+$e$^-$ pair production, $0^+ \to 0^+$ (Fig. 2). The reaction rate is related to the properties of the Hoyle-state via [15]

$$< \sigma v >\propto \frac{\Gamma_\alpha \Gamma_{rad}}{\Gamma} \exp(-E_R/k_B T) \tag{3}$$

where Γ, Γ_α and Γ_{rad} are the total width and α and radiative partial widths, with $\Gamma_{rad} = \Gamma_\gamma + \Gamma_{e^+e^-}$. E_R is the energy of the Hoyle-resonance above the ^{8}Be+^{4}He threshold. In Section 5.2 we discuss the current measured values of the total and partial widths of the Hoyle-state. Since, to a good approximation, $\Gamma = \Gamma_\alpha$ then the proportion of times the Hoyle-state decays to the ground state of carbon-12 is given by the ratio Γ_{rad}/Γ. This has a weighted average of $(4.03 \pm 0.10) \times 10^{-4}$ corresponding to a probability for radiative decay to the ground state of 1 part in 2500.

The energy of the Hoyle-state lies 285 keV above the ^{8}Be+α decay threshold. This would correspond to the peak of the Gamow window for temperatures close to 2.5×10^8 K. Again, the presence of the state close to the critically sensitive region for synthesis of carbon-12 is crucial, providing an enhancement by approximately 7-8 orders of magnitude [3]. A few hundred keV higher in energy and the dominant influence of the state would effectively be lost.

Critically, the energy production at temperatures close to 10^9 K is proportional to T^{41} (T being temperature) and hence the triple-α process occurs most strongly in the highest temperature regions of the star; and is predominantly responsible for the luminosity of red giants [15].

The ratio of carbon to oxygen observed in the Universe is C/O=0.6. Just as it is crucial that there is a resonance at the right energy to synthesise ^{12}C at 2×10^8 K, it is equally important that there is not a similar resonance in ^{16}O to destroy the carbon, as it is manufactured, through the ^{12}C(α,γ)^{16}O

5

reaction. In the case of ^{16}O the presence of the 7.117 MeV, 1$^-$ state, just below the 7.16 MeV α-decay threshold and the 8.87 MeV, 2$^-$, state being unavailable due to it having unnatural parity, is perhaps just as fortuitous as the Hoyle-state having the *right* energy. In any case, it is unlikely that nature would have found a way to construct the observed universe without the precise arrangement of states in ^{8}Be, ^{12}C and ^{16}O.

The theoretical calculation of the reaction rate of the 3α reaction has in the last five years been intensely debated. This development started by a calculation using a continuum-discretized coupled channels method (CDCC), which predicted much higher reaction rate at temperatures below 10^8 K than previous calculations [18]. This result has triggered a number of new calculations using a range of calculating techniques, including hyper-spherical harmonics expansions [19], extended Breit-Wigner formalism [20], Faddeev equations [21], and an imaginary time method [22]. While there is still considerable variations between the reaction rate calculated by the different methods, there is now a consensus that the result from the CDCC calculation overestimated the low-temperature rate by many orders of magnitude. It turns out that the different calculations also predict different α-decay of the Hoyle-state, and this can therefore be used to provide some experimental insights into the validity of the different calculations. This will be discussed further in section 5.2.

It is interesting to note that Hoyle's original line of work related to using the observed elemental abundances to infer contraints on the reaction rate for forming ^{12}C is still being pursued. As an example Austin, West and Heger have used the abundances of elements predominately produced in core collapse supernovae to infer effective reaction rates for the 3α and ^{12}C$(\alpha,\gamma)^{16}$O reaction rates, and then used these rates to more reliably predict the abundance of ^{11}B to constrain the neutrino emission from supernovae [23].

3 Theoretical approaches and models of ^{12}C and the Hoyle-state

A variety of models have been deployed to try and understand the structure of states in light nuclei and in particular ^{12}C. These vary tremendously in both character and complexity. At the single particle limit there lies the nuclear shell model. Such calculations, for example those of Ref. [24], reproduce rather well the energy of the first 2$^+$ (4.44 MeV) excitation, illustrating the overlap of this state, together with that of the ground-state, with the independent particle limit. However, in the region of the second 0$^+$ state (0$_2^+$), the Hoyle-state, there is a void in such calculations; the energy of this state cannot be reproduced within this shell-model description.

This lack of ability of the shell model to reproduce the energy of the Hoyle-state has been taken as a signature of an alternative structure. This strongly resonates with the ideas articulated in Section 1, where the Ikeda prescription suggests that states close to α-decay thresholds could have a well-developed α-cluster structure [12]. As such, the simple shell model basis would not be sufficient to capture such structural modes.

An alternative approach is to use methods which explicitly include the α-particle clusters together with an appropriate α-α interaction. The spirit here is very similar to the earlier ideas of Hafstad and Teller [11] (Section 1).

3.1 *The Alpha Cluster Model*

The Alpha Cluster Model (ACM) was first conceived of by Margenau [25] and then further developed by Brink [26, 27]. The principle construction of the alpha particle model is that quartets are produced from pairs of protons and neutrons which are coupled to a total angular momentum of zero, i.e. they

6

may be represented by a relative 0s-state. The wave-functions of such quartets may then be written as

$$\phi_i(\mathbf{r}) = \sqrt{\frac{1}{b^3\pi^{3/2}}} exp\left[\frac{-(\mathbf{r}-\mathbf{R}_i)^2}{2b^2}\right] \tag{4}$$

Here $\mathbf{R}_i$ is the vector describing the location of the ith quartet, and $b = (\hbar/m\omega)^{1/2}$ is a scale parameter which determines the size of the α-particle.

Even though the α-particle is a boson its constituents are fermions, and hence the overall wave-function of the system, formed from the collection of α-particles, must then be antisymmetrized. The $N\alpha$ wave-function is thus achieved by using a Slater determinant

$$\Phi_\alpha(\mathbf{R}_1, \mathbf{R}_2, ..., \mathbf{R}_N) = K\mathcal{A}\prod_{i=1}^{N}\phi_i(\mathbf{R}_i) \tag{5}$$

$\mathcal{A}\prod_{i=1}^{N}\phi_i(\mathbf{R}_i)$ being the Slater determinant wave-function ($\mathcal{A}$ is the antisymmetrization operator accounting for the Pauli Exclusion Principle - recognising the fermionic degree of freedom) and K a normalisation constant. At short distances the antisymmetrization serves to break the α-particles, whereas for large α-particle separations they retain their bosonic identity. Thus, as the α-particles are squeezed together, which occurs as the excitation energy falls below the 3α-decay threshold in ^{12}C, the wave-function will contain less of the original α-particle structure. Though, the α-particle structure may be broken, it is possible that the symmetry associated with the 3α-structure is retained. Correspondingly, one would expect the ground-state of ^{12}C to contain the 3α symmetry, but not necessarily the α-particle clusters (see Fig. 6 for an illustration of this point using the more sophisticated AMD approach). The Hoyle-state lies above the α-decay threshold and thus has the possibility for attaining a 3α-cluster structure (again illustrated by Fig. 6).

The Hamiltonian describing the total energy of the $N\alpha$-system is

$$H = \sum_{i=1}^{A}T_i + \frac{1}{2}\sum_{i\neq j}[v(\mathbf{r}_i-\mathbf{r}_j) + v_c(\mathbf{r}_i-\mathbf{r}_j)] - T_{c.m.} \tag{6}$$

$T_{c.m.}$ is the center-of-mass energy and the α-α interactions are governed by the effective interaction potential $v(\mathbf{r}_i-\mathbf{r}_j)$ and Coulomb interaction $v_c(\mathbf{r}_i-\mathbf{r}_j)$.

The optimal geometric arrangement of the α-particles is arrived at by varying the locations and size of the α-particles and minimising the energy computed via Equation 6. This model has been applied extensively to light cluster systems by for example Brink [26, 28]. In the case of ^{12}C the alpha-cluster model finds two structures, the first is an equilateral triangular arrangement which historically has been associated with the ground-state, the second is a linear arrangement (or chain) which was originally linked to the Hoyle-state. The latter conjecture coincides with the ideas of Morinaga who had suggested that the 7.65 MeV state in ^{12}C might be a linear arrangement of 3α-particles [29]. Based on this structure he predicted a rotational band with 2^+ members at 9.7 MeV and 4^+ at 14.18 MeV. Although their spin and parity were unknown at the time, there were known states at 9.61 MeV and 14.16 MeV which were possible candidates. It was noted that the width of the 9.61 MeV state was not consistent with such an explanation and indeed it transpired that the spin and parity was 3^- and the 14.16 MeV state was the 4^+ member of the ground state rotational band. The existence, or otherwise, of the 2^+ excitation remained unanswered until recently (see Section 6).

3.2 *Condensates and the THSR wave-function*

Given the asymptotic bosonic nature of the 3α-particle system, it is possible that for the Hoyle-state the separation of the clusters is such that the internal structure of the α-particle is no longer so important.

7

The conditions necessary to achieve this require that the nuclear radius is sufficiently large; which may be achieved close to the α-decay threshold, where in a state which marginally unbound, an α-particle may tunnel significantly into the barrier increasing the nuclear volume. Electron inelastic scattering measurements [30] indicate that the Hoyle-state is associated with a radius larger than that of the ground state by a factor of 1.35 to 1.60 (depending on the model used to analyse the data) which would correspond to an increase in volume by a factor of 2.5 to 4. Under such circumstances it is possible that the antisymmetrizer, $\mathcal{A}$, in equation 5, plays a negligible role and the system may be described as 3 bosons, which in analogy with atomic systems may form a condensate. Thus, the Hoyle-state has been connected with a Bose Einstein Condensate (BEC) of α-particles [31, 32, 33, 34].

In order to describe such a possibility, the Bloch-Brink wave-function (Section 3.1) has been adapted by Tohsaki, Horiuchi, Schuck and Röpke (THSR) to reflect the possible character of the state [31, 32, 33, 34]. The condensate wave-function thus has a form similar to that of the Alpha Cluster Model

$$\langle \mathbf{r}_1, ...\mathbf{r}_N|\Phi_{n\alpha}\rangle = \mathcal{A}[\phi_\alpha(\mathbf{r}_1, \mathbf{r}_2, \mathbf{r}_3, \mathbf{r}_4)\phi_\alpha(\mathbf{r}_5, \mathbf{r}_6, \mathbf{r}_7, \mathbf{r}_8)\phi_\alpha(\mathbf{r}_{N-3}, ..., \mathbf{r}_N)] \tag{7}$$

here the construction is for N nucleons grouped into quartets described by ϕ_α. The wave-function of the resulting α-particle being given by

$$\phi_\alpha(\mathbf{r}_1, \mathbf{r}_2, \mathbf{r}_3, \mathbf{r}_4) = e^{-\mathbf{R}^2/B^2}\phi(\mathbf{r}_1 - \mathbf{r}_2, \mathbf{r}_1 - \mathbf{r}_3, ...) \tag{8}$$

where $[\mathbf{R} = \mathbf{r}_1 + \mathbf{r}_2 + \mathbf{r}_3 + \mathbf{r}_4]/4$ is the c.o.m. coordinate of one α-particle and $\phi(\mathbf{r}_1 - \mathbf{r}_2, \mathbf{r}_1 - \mathbf{r}_3, ...)$ is a Gaussian wave-function, or wave-packet

$$\phi(\mathbf{r}_1 - \mathbf{r}_2, \mathbf{r}_1 - \mathbf{r}_3, ...) = \exp\left(-[\mathbf{r}_1 - \mathbf{r}_2, \mathbf{r}_1 - \mathbf{r}_3, ...]^2/b^2\right) \tag{9}$$

as in the ACM b is the size parameter of the *free* α-particle and B ($\gg b$) is the parameter which describes the size of the common Gaussian distribution of the, in the case of ^{12}C, three α-particles. In the limit that $B \to \infty$ then the antisymmetrization operator $\mathcal{A}$ ceases to be important and the wave-function (equation 7) becomes the product of Gaussians, i.e. a wave-function describing a free α-particle gas. The important feature is that in the limit that the volume becomes small the antisymmetrization takes over and the wave-function respects the internal fermionic degrees of freedom. In this way the wave-function is very similar to that of the ACM, but possesses an additional variational degree of freedom. It is this flexibility that makes this ansatz for the wave-function so powerful.

One of the main successes of this model is that it manages to reproduce the charge form factor for the electron inelastic excitation from the ^{12}C ground-state to the Hoyle-state without any arbitrary normalisation [31] as shown in Fig. 3. The strong agreement with the data is a clear indication of the nature of the Hoyle-state as being both spatially extended and strongly influenced by an internal α-particle structure of ^{12}C.

A key feature of the THSR approach is that the decomposition of the THSR Hoyle-state wave-function into the single particle α-particle orbitals reveals that there is a 70% overlap of the THSR wave-function with 3 α-particles in S-orbital (the lowest energy state within the potential defined by the mutual interaction), confirming that at least at this level the α-particles retain their asymptotic properties (see Fig. 4). On the other hand the ground-state is fragmented into components with roughly equal S, D and G amplitudes [35, 14]. This demonstrates the strong influence of the Pauli Exclusion Principle (PEP) in breaking the α-particles in the ground state. The fact that in the Hoyle-state there is 30% contribution from orbitals other than the S-state indicates that the PEP still plays a small role in the Hoyle-state in the interior region where the α-particles still have a small overlap.

Consequently, to first order the α-particles can be viewed as all residing in the lowest energy state, S-state, of the potential which stems from their mutual interaction. Excitations then are associated with the α-particles being moved from this level to the next possible orbital permitted by the symmetry of the systems; a D-state. The BEC model predicts the corresponding 2^+ excitation of 9.4 MeV with a width of 0.6 MeV [33, 36]. Interestingly, this model predicts analogues of the Hoyle-state in the 4α-system ^{16}O which would indicate the 15.1 MeV state may have a condensate structure [14].
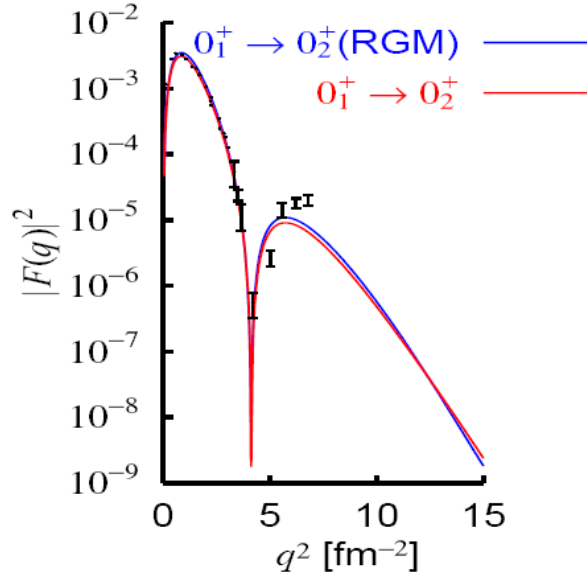
Figure 3: The calculated inelastic form factor for electron inelastic scattering from the 0^+ ground state to the 0_2^+ excited state [31] for the BEC approach (red), compared with the experimental data from [30].
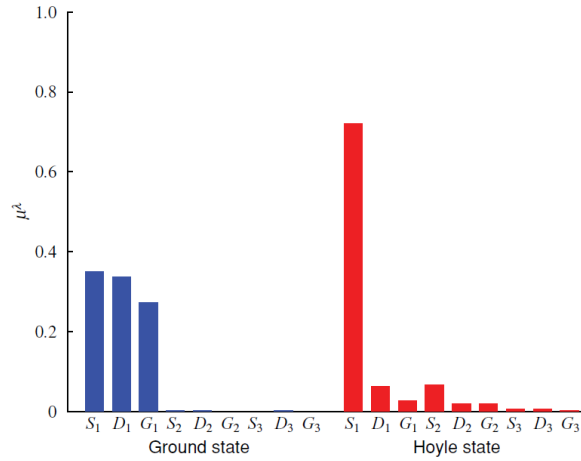

Figure 4: Occupation of the α-particle orbitals associated with the Hoyle-state of ^{12}C compared with the ground state, from [35, 14].
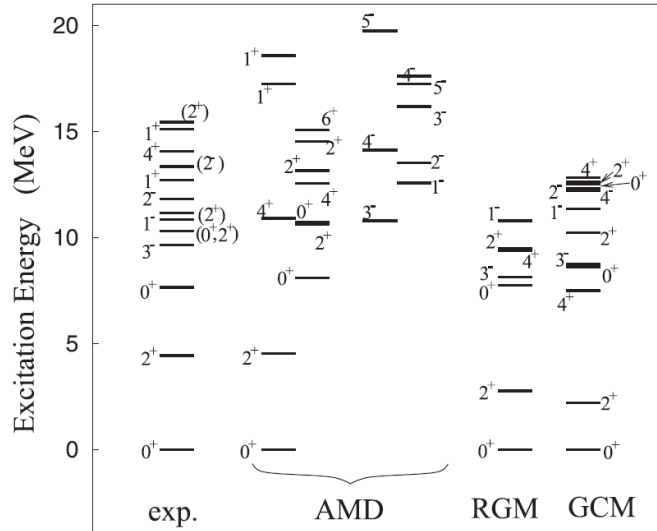
9

Figure 5: Energy levels for ^{12}C predicted by the AMD approach [38], resonanting group method (RGM) [39] and generator coordinate method (GCM) [40], from [38].

3.3 *Antisymmetrised Molecular Dynamics (AMD) and Fermionic Molecular Dynamics (FMD)*

The AMD approach, which has been comprehensively reviewed recently by Kanada-En'yo and Horri-uchi [37], has many important advantages over microscopic cluster models, but the most significant is that there are no assumptions made about the existence of clusters or the relative coordinates between clusters. The model is one which the nucleonic degrees of freedom are explicitly included and the A-nucleon wave-function is then antisymmetrised, again, via a Slater determinant;

$$\Phi_{AMD}(\mathbf{Z}) = \frac{\mathbf{1}}{\sqrt{\mathbf{A}!}}\mathcal{A}\{\varphi_{\mathbf{1}}, \varphi_{\mathbf{2}}, ..., \varphi_{\mathbf{A}}\} \qquad (10)$$

The model resembles the Bloch-Brink cluster model, but contains as degrees of freedom the nucleons and releases the constraint that α-particles be preformed. Consequently, clusters naturally emerge without being imposed. The φ_i are Gaussian wave-packets in space, $\phi_{\mathbf{X}_i}(\mathbf{r}_j) \propto \exp(-\nu(\mathbf{r}_j - \mathbf{X}_i/\sqrt{\nu})^2)$, but also possesses spin (χ_i) and isospin character (τ_i); $\varphi_i = \phi_{\mathbf{X}_i}\chi_i\tau_i$. The energy of the system is computed, variationally, utilizing an *effective* nucleon-nucleon interaction. The flexibility of this approach allows a suitable description of cluster and shell-model type systems, alike, and the structure emerges naturally from the details of the nucleon-nucleon interaction under the guidance of the Pauli Exclusion Principle.

The model provides a good description of the spectrum of states in ^{12}C as revealed in Fig. 5 [38] where the more shell model like states such as the first 2^+ state are well reproduced equally as the Hoyle cluster like state. Fig. 5 shows a comparison with the experiment and more traditional cluster models (RGM and GCM). These latter models reproduce some of the features of the states above the threshold, where clustering is strong, but fail to reproduce the energy of the first 2^+ state.

The densities shown in Fig. 6 reveal the underlying intrinsic structures of the first three 0^+ states (and first three 2^+ and 4^+ states). The ground-state is clearly quite compact, and although the cluster symmetry is present, the identity of the α-particles is suppressed. The Hoyle-state, 0_2^+, is clearly much more extended with a loose assembly of α-particles. The 2^+ and 4^+ states which might be associated with collective excitations, do not show the same intrinsic structure illustrating that a rotational model may not be the appropriate description of the collective modes. The 0_3^+ state shows the same characteristics

10
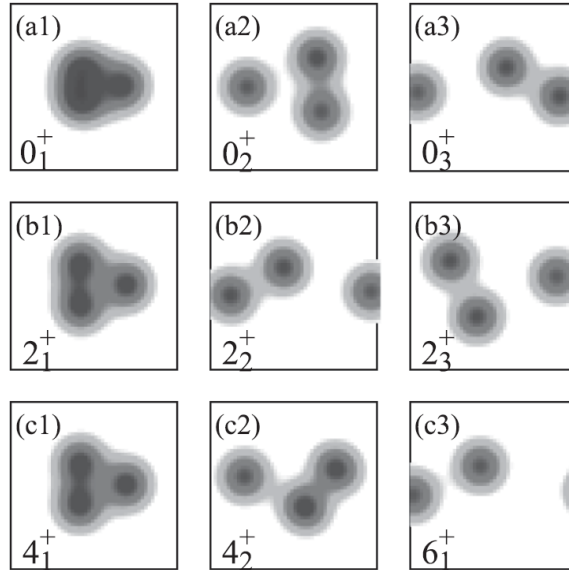
Figure 6: AMD densities of the ground state band, 0_1^+: a1, b1 and c1, Hoyle-band, 0_2^+ a2, b2, c2 and 0_3^+ band a3, b3, c3, from [38].

but even more exaggerated.

An alternate approach to AMD which contains an additional degree of freedom, namely the width parameter of the Gaussian wave-functions, is fermionic molecular dynamics (FMD) [41]. The features of these calculations essentially coincide with those of the AMD, but the variable gaussian width should allow, in principle, an even better description of shell-model like states and those of weakly bound systems.

The FMD description provides a good reproduction of the charge form factor for elastic and inelastic electron scattering associated with the 0_1^+ and 0_2^+ states, respectively. Fig. 7 shows a comparison of the FMD results with those of the Alpha Cluster Model (ACM) and the THSF wave-function (BEC) together with the corresponding charge densities. All models show an increased radius for the Hoyle-state and reproduce the data reasonably well. For the Hoyle-state, the conclusions of the FMD are similar to those of the AMD approach and are illustrated in Fig. 8. Here the Hoyle-state cannot be reproduced by a single intrinsic structure, but rather a superposition of 3α arrangements are required, as might be expected for a state which resembles an α-particle gas (the first four images). The ^{12}C ground-state, conversely, has a single dominant configuration (fifth image). The FMD approach predicts the energy of the Hoyle-state to be 9.50 MeV and the 2^+ excitation to be at 11.83 MeV [42], an energy separation of just over 2 MeV.

3.4 *Ab initio approaches*

Rather than a starting point of effective interactions, ab initio approaches attempt to build the nuclear properties from the first principles of bare nucleon-nucleon interactions. In this instance, the only bound configuration of two nucleons is the n-p system in the spin triplet state. The binding of the neutron and proton in the spin triplet state, S=1, compared to the spin singlet case, S=0, owes its origins to the Tensor component of the strong interaction, which in turn may be traced to both scalar (pion) and vector (ρ) meson exchange. Understanding how to embed the detail of the nucleon-nucleon interaction, which arises from the understanding of the n-p system and nucleon-nucleon scattering measurements, into the computation of the properties of a nucleus is a significant challenge.
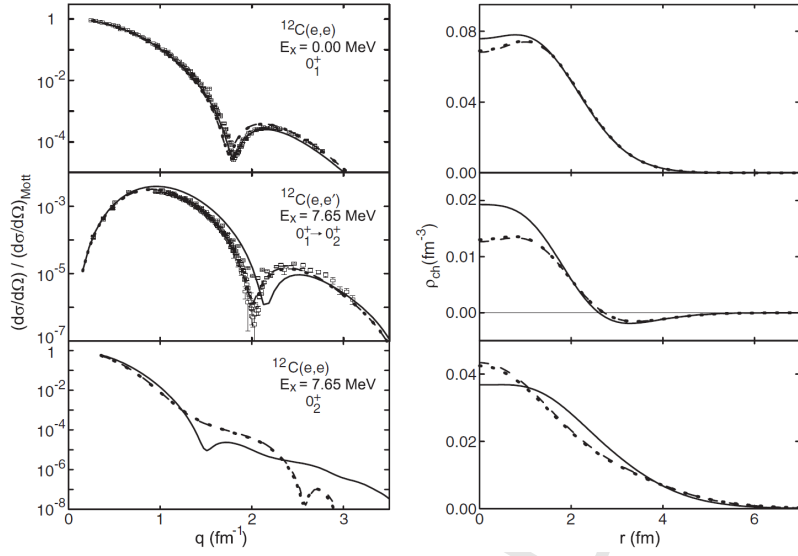
Figure 7: Left: FMD (solid lines), α-cluster (dashed lines), and BEC (from [31], dotted lines) predictions of the charge form factors in ^{12}C are compared with the experimental data (open squares) [30]. Elastic scattering on g.s. (top), transition to the Hoyle-state (middle), and the fictional elastic scattering on the Hoyle-state (bottom). Right: The corresponding charge density distributions.

$|\langle 1|0_1^+\rangle| = 0.30$ $|\langle 2|0_1^+\rangle| = 0.25$ $|\langle 3|0_1^+\rangle| = 0.15$ $|\langle 4|0_1^+\rangle| = 0.08$ $|\langle 5|0_1^+\rangle| = 0.94$

$|\langle 1|0_2^+\rangle| = 0.72$ $|\langle 2|0_2^+\rangle| = 0.71$ $|\langle 3|0_2^+\rangle| = 0.61$ $|\langle 4|0_2^+\rangle| = 0.61$ $|\langle 5|0_2^+\rangle| = 0.04$

Figure 8: Densities of the four FMD with the strongest amplitudes in the Hoyle-state and their respective amplitudes for the ground state (0_1^+) and the Hoyle-state (0_2^+). The fifth density plot is the leading component in the ground state. [42].

This partially arises from the fact that single meson exchange does not capture the full complexity of the nucleon-nucleon interaction, and higher order exchanges can have a major contribution, but that three body terms (and may be to a lesser extent higher order terms) play a significant role. One way of capturing such contributions is through processes such as the Fujita-Miyazawa [43] type exchanges, in which a nucleon can get excited via a pion exchange, which then alters the nature of the interaction of this excited nucleon with further nucleons. The parameterisation of the nuclear force based upon such interactions has led to a rather successful description of the properties of the binding energies and spectroscopy of light nuclei up to A=12, for example through the Greens Function Monte Carlo approach [44, 45, 46]. However, in such approaches there are a number of challenges; including the mass range of nuclei that can be reached and that the choice of parameterisation of the two-body interaction leads to ambiguities in the nature of the 3-body force – there is no unique 3-body interaction.

An alternative approach which recognises that ultimately the nuclear strong force emerges from the QCD degrees of freedom, and that the meson exchange is a manifestation of this, is to use Chiral Perturbation Theory (ChPT) [47]. The QCD description is simplest where the strong coupling constant, α_S, is weakest. At low energies, that are appropriate for nuclear matter, the regime is such that the coupling is so strong that it cannot be treated as a perturbation - the non perturbative regime. One approach to circumvent this has been to calculate properties based upon constituents being fixed on a latti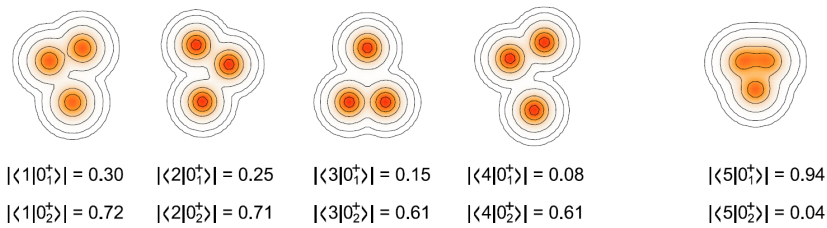ce (lattice QCD). A second approach has been to use an effective field theory which draws on ideas developed for solid state theory - Chiral Effective Field Theory (ChEFT) [47]. This theory draws on the fact that the up and down quarks display a chiral-like symmetry which is broken only by their non-zero mass. In this description the properties of both the hadrons (including protons and neutrons) and the mass of the pion emerges. In analogy with condensed matter chiral-symmetry breaking the pion should be a spinless Goldstone boson, and which couples only weakly. This last aspect is rather essential as it then permits a tractable, perturbative, approach [47].

This effective field theory then results in a series of exchange diagrams which relate to the perturbative expansion in orders of $(Q/\Lambda)^n$, where Q is of the order of the pion mass ($\sim$140 MeV) and Λ is the chiral symmetry breaking scale ($\sim$1 GeV). In leading order (n=0) there is a one-pion exchange component plus what is called a contact term, which in essence accounts for the heavier exchange mesons (ρ, σ and ω) whose range is significantly less than that of the pion. The next term (n=1) vanishes due to parity and time-invariance, leaving the $n = 2$ term as the next to leading order, NLO. This includes processes such as two-pion exchange. The complexity increases as more orders are added which means that although the contribution from each term to the interaction is less by the factor (Q/Λ) there are more processes to consider. The aim is to calculate the interaction to all orders, but this is clearly a challenge, and NNNLO is the current milestone (N^{3}LO).

The great advantage of this approach is that 3-body forces emerge naturally, first appearing in the NNLO term, and that higher order terms such as NNNLO introduce 4-body interactions. Here the two-body and n-body interactions emerge in a consistent fashion.

Such developments offer the opportunity to develop an interaction which may be applied to the description of nuclei whose degrees of freedom may at least be traced to QCD, even if they are not explicitly those of QCD. The N^{3}LO interaction has been applied through models such as the No Core Shell Model (NCSM) [48]. Here the complexity of the interaction is traded against the simplicity of the basis in which the interaction is applied. The states adopted in this approach are those of the harmonic oscillator (HO), which are attractive due to their analytic form.

The NCSM has been extremely successful in terms of the reproduction of the spectroscopy of a range of light nuclei. However, has been famously unsuccessful in the reproduction of one particular state in ^{12}C - the 7.65 MeV, 0^+, Hoyle-state [49]. In order to capture the detail of this state, or more precisely its experimentally observed excitation energy, nucleons must be scattered into very high-lying levels within the HO potential. This feature may indicate that the HO basis is for some reason inappropriate in its attempt to capture the structural properties of this state. The harmonic oscillator basis is not

ideally suited to the reproduction of the behaviour of weakly bound systems, as the asymptotics of the wave-functions do not match well the strong exponential character of the tails of wave-functions for states close to threshold.

It has been argued that this reflects the 3α-cluster structure of this state. However, it should be noted that the highly clustered nucleus ^{8}Be is well-described within the ab-initio NCSM [50]. This ability to reproduce the ground state energy of ^{8}Be, albeit with a model space of 6-8 $\hbar\omega$ and not the Hoyle-state is curious. This may be partially responsible for the fact that in order to capture the ground state energy of ^{8}Be, whose properties are dominated by the $1p$-levels, 6-8 $\hbar\omega$ excitations are required. Similarly, if the Hoyle-state is associated with a $(1s)^4(1p)^4(1d)^4$ configuration then it too would be expected to be reasonably reproduced by the NCSM. This configuration would most naturally be associated with a linear arrangement of 3α-particles [51]. This lack of reproduction of the experimental energy of 7.65 MeV by the NCSM may point to a rather different structure (i.e. not a linear arrangement). There has been a recent attempt at capturing the structure of the Hoyle-state in the NCSM using a symmetry guided selection of most important contributions and a more effective interaction [52]. This calculation concludes that to capture the Hoyle-state requires excitations up to 18 $\hbar\omega$.

The ChEFT interaction has been exploited in lattice type calculations to compute the properties of both the ^{12}C ground-state and Hoyle-state [53, 54]. These calculations considered the individual nucleons, but their locations were constrained to a cubic lattice. The lattice spacing was rather coarse (1.97 fm) on the scale of the size of an alpha-particle, but the absolute binding energies of the states were remarkably well reproduced. The overall conclusion was, again, that the Hoyle-state was associated with a more extended structure than the ground state, and interestingly though it could be accommodated within the geometry of the lattice, the chain structure (linear arrangement) of alpha-particles was not preferred. To provide a deeper insight, a finer lattice mesh is clearly required, but this is an exciting development.

3.5 *Dynamical symmetries associated with the 3α cluster structure of ^{12}C*

Even back in 1938 Hafstad and Teller [11] suggested the nature of the dynamical symmetries associated with the 3α cluster structure of ^{12}C. In this instance one can link them to a classical spinning top with a triangular point symmetry. In other words, a spinning triangle which can rotate around its symmetry axis, but also wobble as it spins – just as a spinning coin in its final moments before coming to rest. The quantal rotational properties of such a system is given by the equation

$$E_{J,K} = \frac{\hbar^2 J(J+1)}{2\mathcal{I}_{Be}} - \frac{\hbar^2 K^2}{4\mathcal{I}_{Be}} \tag{11}$$

Here $\mathcal{I}_{Be}$ is the moment of inertia corresponding to two touching α-particles, which may be determined from the rotational band associated with the ^{8}Be ground-state [11]. Based on this structure there should be a number of rotational bands with different values of K; the projection of the angular momentum onto the 3-fold symmetry axis. For $K^\pi=0^+$, this projection is thus zero and the rotations will be around an axis which lies in the plane of the three α-particles (in fact passing through the centre of one α-particle and bisecting the other two), generating a series of states 0^+, 2^+, 4^+ .... These correspond to the rotation of a ^{8}Be nucleus (two touching α-particles). The next set of rotations are associated with the rotation around an axis perpendicular to the plane of the triangle, with each α-particle having one unit of angular momentum - giving $L = 3 \times 1\hbar$; $K^\pi=3^-$. Rotations around this axis and that parallel to the plane combine to give a series of states 3^-, 4^-, 5^-.... The next set of collective states then correspond to each α-particle having $L = 2\hbar$; $K^\pi=6^+$, corresponding to $L = 3 \times 2\hbar$.

These rotations may be associated with an object with a D_{3h} point group symmetry. Superimposed on this rotational behaviour, vibrational modes are also possible. The corresponding rotational and
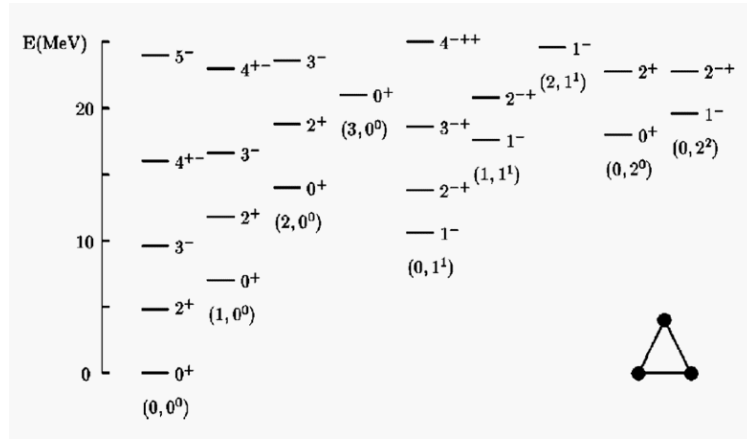
14

Figure 9: Spectrum of the energy levels of an equilateral triangle configuration. The bands are labeled by $(v_1; v_2^l)$ [57].

vibrational spectrum can also be described by a form [55, 56, 57]

$$E = E_0 + Av_1 + Bv_2 + CL(L+1) + D(K \pm 2l)^2 \qquad (12)$$

where $v_{1,2}$ are vibrational quantum numbers, and v_2 is doubly degenerate; $l = v_2, v_2 - 2, 1$ or 0, L is angular momentum, and its projection is K on a body-fixed axis [57]. A, B, C and D are adjustable parameters. The spectrum of states predicted by the choice $A = 7.0$, $B = 9.0$, $C = 0.8$ and $D = 0.0$ MeV is shown in Figure 9 [57].

Here the states correspond to different values of K ($K = 3n$, $n = 0, 1, 2...$) and L. For $K=0$, $L=0, 2, 4$ etc....., which is a rotation of the plane of the triangle about a line of symmetry, whereas for $K > 0$ $L = K, K + 1, K + 2.....$ In the present case, $K=0$ or 3 is plotted with the parity being given by $(-1)^K$. The $K=0$ states coincide well with the well-known 0^+ (ground-state), 2^+ (4.4 MeV) and 4^+ (14.1 MeV) states. The $K=3$ states, as described above, correspond to a rotation about an axis which passes through the center of the triangle. The first state has spin and parity 3^- and coincides with the 9.6 MeV, 3^-, excited state. The next such would be $K=6$, $J^\pi=6^+$. A prediction of this model is that there should be a 4^- state almost degenerate with the 4^+ state. Recent measurements involving studies of the α-decay correlations indicated that the 13.35 MeV unnatural-parity state possessed $J^\pi=4^-$ [58, 59]. The close degeneracy with the 14.1 MeV 4^+ state would appear to confirm the D_{3h} symmetry.

In this model the Hoyle-state would then correspond to a vibrational excitation of the ground-state $(1,0^0)$ - Fig. 9. This could be either of monopole character, where the triangular symmetry present in the ground-state becomes fully developed into a 3α-cluster structure, or that the triangle opens into a linear configuration - the 3α chain. In the picture of Bijker and Iachello [57] the triangular symmetry is retained, and the symmetries associated with the Hoyle-state would be similar to those of the ground state giving the same sequence of excitations; 0^+, 2^+, 3^-,....

In principle, this ambiguity can be resolved experimentally by determining the rotational properties of the Hoyle-state, i.e. from a measurement of the energy of the 2^+ and 4^+ excitations from which the moment of inertia of the underlying structure may be obtained. This, of course, relies on the state possing rotational excitations. There are alternative possibilities due to the presence of the bosonic α-particles, yielding a bosonic condensate or α-particle gas.

15

3.6 *Summary*

When it comes to the Hoyle-state, the common feature of these models is that they universally indicate a strongly developed cluster structure, where α-particle correlations play a significant role. The determination of the nature of the alpha-particle structure, be it a Bose α-particle gas or condensate, or a geometric arrangement of α-particles, and if so how the α-particles are arranged, requires an understanding of the excitations of the Hoyle-state. This is the area of research which has seen the most dramatic progress most recently (Section 6). All of the models explored here indicate an extended structure for the Hoyle-state compared with the ground-state of ^{12}C. In the BEC, ACM, FMD and AMD approaches the radius of the ground-state is found to be 2.40, 2.40, 2.39 and 2.53 fm, respectively, whereas for the Hoyle-state they are 3.83, 3.71, 3.38 and 3.27 fm, respectively [42, 38].

4 Continuum and potential effects

A feature of the Hoyle-state is that it resides above the threshold for decay into both ^{8}Be+α and 3α. As a consequence it resides at an energy where the continuum plays a role. This feature underpins a deeper question and that is related to the appearance of cluster states close to, or slightly above, decay thresholds - the Ikeda picture [12]. The appearance of cluster states at thresholds is well documented [58], but just because a threshold appears does not necessarily mean that a state with cluster structure should also. However, weakly bound nuclei close to decay thresholds can be thought of as open quantum systems where the properties of the unbound states influence, or couple to, the bound states below the threshold. Okołowicz, Nazarewicz and Płoszajczak have recently explored the link between the appearance of cluster states at threshold and the role of the continuum [60]. This is also discussed in Ref. [61].

The work of Ebran *et al.* [62] also emphasises that the nature of the interaction, which in turn influences the depth of the mean-field potential, also plays a role in the degree to which clustering is enhanced, or otherwise. A deeper mean-field potential leads to both a concentration of the wavefunction in the nuclear interior and a shorter characteristic wave-length. This has the effect of increasing the intensity of the densities associated with the clusters and a stronger cluster identity.

5 Observable properties of the Hoyle-state

In this section we will review a selected range of experimental probes used to gain information on the Hoyle-state. A more general review of experimental aspects of nuclear cluster physics is provided in a recent volume [63].

In Fig. 10 we illustrate possible routes for population and decay of the Hoyle-state. The open decay channels are the 3α-decay and the electromagnetic decay either via a cascade through the lower lying 2^+ state, or, directly with an E0 transition to the ground state. The α-decay is to a three-particle final state, and therefore the final state distribution of the α-particles is not uniquely given by kinematical conservation laws. Consequently, it is not only the partial width for α-decay, but also the α-decay final state distribution, which must be determined. The Hoyle-state is populated using many probes, including transfer reactions, scattering reactions, and weak and electromagnetic transitions. These probes will be discussed in individual sections below.

It may be worth emphasising that any knowledge of the structure of the Hoyle-state can only come from confronting these observables with nuclear structure models. In doing this, it is the goal to extract information such as the degrees of α-clustering, the correlations between the α-particles, the spatial extension of the state etc.
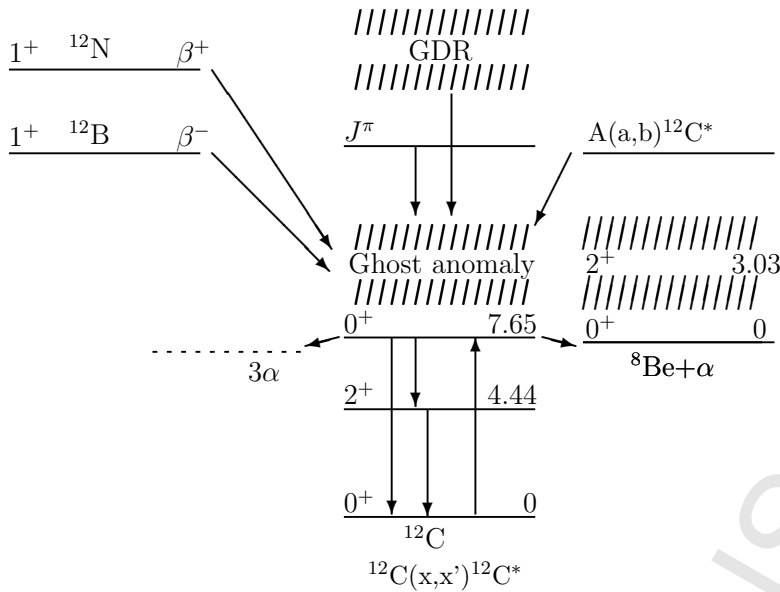
16

Figure 10: Schematic level scheme of ^{12}C including decay channels and methods of populating the Hoyle-state discussed in the text.

5.1 *Energy and width*

The most recent evaluations of the observable quantities discussed in the following are collected in Table 1 for convenience. The energy and width of the Hoyle-state are among the key parameters needed for a precise determination of the reaction rate of the astrophysical 3α-reaction. Consequently, the experimental determination of these quantities has been the focus of much work, some of which is reviewed by Buchmann and Barnes [64], see also [65, 66, 67], and Section 2 which describes the properties of the Hoyle-state in the stellar synthesis of ^{12}C. The determination of the energy is dominated by the measurement of Nolen and Austin [68] who used proton scattering off ^{12}C and a magnetic spectrometer to precisely, and accurately, determine the energy.

For the width, what is needed in astrophysics is the total radiative width, which is determined via measurements of the total radiative branching ratio ($\Gamma_{\rm rad}/\Gamma$), the pair-decay branching ratio (Γ_{π}/Γ), and the pair-decay width (Γ_{π}). Table 1 presents the measured valued of these three quantities. From these measurements the total radiative width can be extracted, which is required for astrophysics, but also the total width and the partial radiative and alpha-decay widths. These derived quantities are collected in Table 2.

The current best values for the radiative and pair-decay branching ratios are derived from measurements performed in the 1970s or earlier. The quantity with the largest error is the pair-decay branching ratio. Several groups are pursuing measurements to improve this number, e.g. [69]. There are also plans to extract the pair-decay branching ratio via measurements of the relative pair-decay branching ratios of the E0 ground state and E2 cascade decays [65]. The same group also pursues an improved measurement of the radiative branching ratio [66]. A new measurement of the radiative branching ratio may also result from β-decay experiments as discussed in Section 5.4.

The pair-decay width, extracted via measurements of electron scattering, is the only absolutely measured quantity, and consequently all the other partial widths depend directly on this number. The pair-decay width has been the object of considerable attention in the past decade. In 2005 the electron-

17

scattering data was re-evaluated resulting in a reduction by 15% (corresponding to a change of 2σ) of the deduced pair-decay width [70]. However, in 2010 this re-evaluation was rejected [71]. This study combined new data from the Darmstadt S-DALINAC and a reanalysis of existing data using the Distorted-Wave Born Approximation to give a new value of $\Gamma_\pi = 62.3(20)$ μeV. In Tables 1 and 2 we have used this value to derive our estimates of all other partial widths.

5.2 α-decay

From the widths given in Table 1, the α-decay rate can be taken as the total decay rate since the electromagnetic partial widths are well within the quoted error of the total width. As for any α-decay the decay rate can be used to extract a spectroscopic factor, or probability to find an α-particle in the nucleus (though strictly speaking spectroscopic factors are not experimentally observable factors and require reference to a model [72]). For light nuclei this analysis is most appropriately performed using the R-matrix formalism, see e.g. Ref. [73] for a more in-depth discussion of the extraction of spectroscopic factors from R-matrix fits.

We use the single level, single channel, R-matrix level profile

$$\rho_\lambda(E) = \frac{P(E)\gamma_\lambda^2}{[E_\lambda - E - (S(E) - B)\gamma_\lambda^2]^2 + [P(E)\gamma_\lambda^2]^2} \ . \tag{13}$$

Here P, S and B are the penetrability, shift function and boundary parameter and E_λ and γ_λ are the level energy and width parameters. Note, the use of this formula for the Hoyle-state assumes that the α-decay is exclusively a two-body process ^{12}C$\rightarrow \alpha+^8$Be; we will discuss the validity of this assumption later in this section.

Barker and Treacy discuss how to choose the width parameter γ_λ corresponding to a given observed width [74]. This relationship between the width parameter and the level width has the property that for a given radius there is a maximum possible level width in the limit of large width parameters γ_λ. This maximum level width increases with radius. In order to reproduce the width of the Hoyle-state one has to use an unusually large radius: with a radius of 1.6 $fmA^{1/3}$ a width of 9.3 eV corresponds to a dimensionless reduced width, $\theta^2 = \gamma_\lambda^2 M_{red} R^2/\hbar^2$ as large as 1.5. In other words, the width of the Hoyle-state is very large when its proximity to the threshold is taken into account, and the large width can only be understood if there is a large degree of α-clustering; this was already noted in [74]. However, from the observed width the radius and the dimensional reduced width can not be individually determined.

Related to the understanding of the width of the Hoyle-state in R-matrix theory, is the concept of the "ghost anomaly". This idea, which was first discussed by Barker and Treacy in 1962 [74], applies to levels positioned close to thresholds where the energy dependence of the width due to the (exponential) rise in the probability to penetrate the potential barrier (in R-matrix formalism this is governed by $P(E)$) gives rise to a secondary peak in the level profile. It is this secondary peak which is called a "ghost anomaly" [74].

Figure 11 shows Equation 13 for the Hoyle-state using level widths of 8.4 eV, 9.3 eV, and 10.2 eV. It is apparent that in addition to the narrow peak there is a secondary peak around 2 MeV above the 3α-threshold. The ratio of the area under the narrow peak and the broad ghost anomaly is of the order 10:1. The ghost anomaly is also indicated in Figure 10. Evidence for the existence of this effect will be further discussed in Section 5.4.

Next we will discuss the assumption of the sequential α-decay sequence ^{12}C$\rightarrow \alpha+^8$Be. The experimental signature for sequential decay is either a peak in the relative energy between two of the α-particles corresponding to the ground state energy of ^{8}Be, or a peak in the single-α spectrum corresponding to the first emitted α-particle populating the ^{8}Be ground state. While the dominance of sequential decay was already demonstrated by Cook *et al.* [5], a quantitative upper limit for non-sequential α-decay of

18

Table 1: Summary of measurements of radiative branching ratio, pair-decay branching ratio, and pair-decay width of the Hoyle-state.

Radiative branching ratio $\Gamma_{rad}/\Gamma \times 10^4$		Pair-decay branching ratio $\Gamma_\pi/\Gamma \times 10^6$		Pair-decay width $\Gamma_\pi \times 10^{-5}$ eV	
Alburger (1961) [86]	3.3(9)	Alburger (1960) [94, 95]	6.6(2.2)	Fregau (1956) [99]	6(3)
Seeger (1963) [87]	2.8(3)	Obst (1972) [96][b]	6.9(2.1)	Crannell (1964) [100]	6.5(7)
Hall (1964) [88]	3.5(1.2)	Robertson (1977) [97]	6.0(1.1)	Gudden (1965) [101]	7.3(1.3)
Chamberlin (1974) [89]	4.2(2)	Alburger (1977) [98]	7.1(8)	Crannell (1967) [102]	6.2(6)
Davids (1975) [90][a]	4.4(2)			Strehl (1968) [103]	6.4(4)
Mark (1975) [91]	4.2(3)			Strehl (1970) [104]	5.9(5)
Markham (1976) [92]	3.9(3)			Crannell (2005) [70]	5.20(14)
Obst (1976) [93]	4.1(3)			Chernykh (2010) [71]	6.2(2)
Recommended	4.03(10) [c]	Recommended	6.7(6)	Recommended[d]	6.2(2)

[a] This value is updated in accordance with ref. 18 in [91].
[b] The value of [86, 95] is superseded by [96].
[c] The recommended value becomes 4.19(11) if the measurement of Seeger and Kavanagh [87] is omitted.
[d] The recommended value assumes the latest analysis of the world data in [71] is correct.
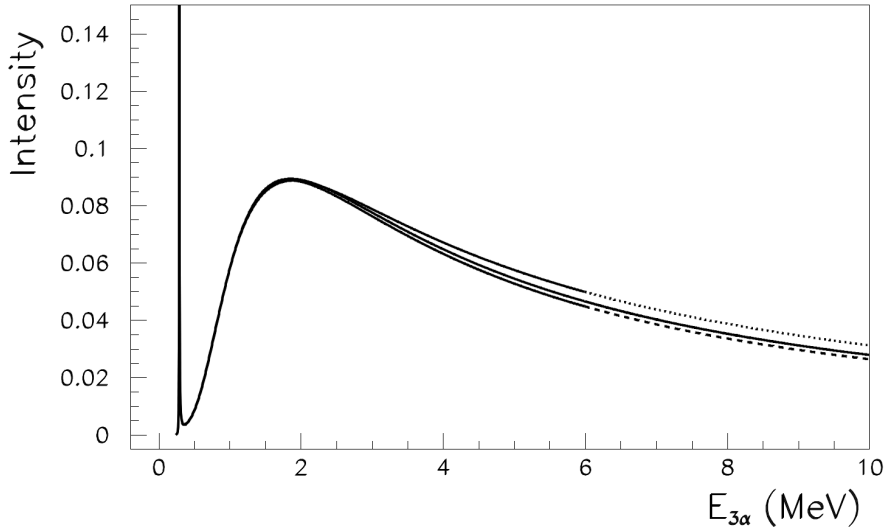
19

Figure 11: Level profile of the Hoyle-state as calculated from Eq. 13 assuming decay into $\alpha+^8\mathrm{Be}(0^+)$. The height of the narrow peak is of the order 10^5. The ratio of the area under the narrow peak and the broad "ghost" contribution is of the order 10:1. The full curve is for a width of 9.3 eV, while the dotted and dashed curved are for width 8.4 eV and 10.2 eV.

4 % was only established as recently as 1994 [75]. In 2011 Raduta *et al.* [76] published a large value of 17 % for non-sequential α-decay, which clearly is in conflict with the previous upper limit. This surprising result has naturally triggered new experimental activity, which has resulted in new, improved, upper limits as low as 5×10^{-3} (95% C.L.) [77, 78], which invalidate the claim for a high non-sequential decay branch. Very recently a new claim for a non sequential decay branch of $9(2)\times10^{-3}$ has been put forward [79], which still needs independent confirmation.

In Section 2 we discussed the issue of the low temperature part of the reaction rate of the 3α-reaction. The experimental information on the α-decay of the Hoyle-state discussed here, supports the conclusion that CDCC calculations [18] over-predicts the non-sequential α-decay branch and therefore also the corresponding contribution to the reaction rate.

An essential question is how to interpret a possible non-sequential decay branch? The ground state of $^8\mathrm{Be}$ is situated only 92 keV above the 2α threshold and it should therefore also host a ghost anomaly, see e.g. Fig. 3 in [80]. It is therefore to be expected that at some level seemingly non-sequential decay branches must exist due to this effect. It is hard to estimate the corresponding branching ratio because the transmission through the Coulomb barrier will depend on the relative energy of two α-particles being either in the peak or the ghost of the $^8\mathrm{Be}$ ground state. The 2^+ first exited state of $^8\mathrm{Be}$ could also contribute to seemingly non-sequential branches. The additional angular momentum barrier will clearly hinder the contribution of this latter channel.

Some authors assume a one-to-one relationship between the final state distribution of α-particles and the structure of the initial state inside the Coulomb barrier. Under this assumption a non-sequential branch could directly result from the structure of the Hoyle-state. As an example Raduta *et al.* [76] argue that, for example, a linear chain structure of the Hoyle-state should result in the centre of the three α-particles being produced at rest and the other two sharing the total energy, while a "condensate" structure of the Hoyle-state should lead to equal energies of the three α-particles.

There has not been much theoretical effort directed towards predicting the 3α decay of the Hoyle-state. In principle this observable should be one of the most sensitive probes of its 3α structure. It
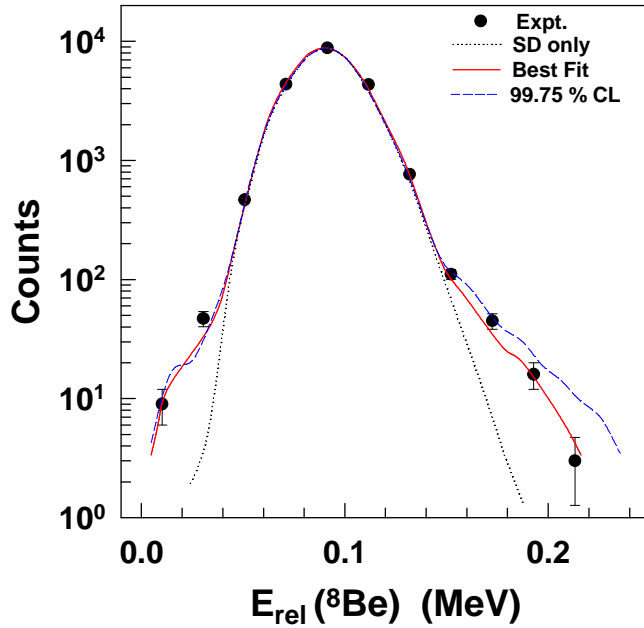
20

Figure 12: Relative energy of two αparticles from complete kinematic measurement of the α-decay of the Hoyle state populated in scattering of 60 MeV α-particles on ^{12}C [79]. The small wings on the tails of the main peak from the ground state of ^{8}Be are interpreted as evidence for non-sequential decay.

is, however, as already alluded to, necessary to understand how the transmission through the Coulomb barrier may modify the relative configuration of the three α-particles. An attempt at achieving this goal using Faddeev equations in a 3α continuum calculation was published by Alvarez-Rodriguez et $al.$ [81]. This calculation is successful at predicting the non-sequential decay branch, with a calculated value of 1%, and it indicates that the change in structure from small to large distances from the decay of the Hoyle-state is very small, and therefore that the final state distribution in this case indeed can be taken as a rather direct probe of its α-cluster structure. R-matrix theory has also been used to characterise the 3α-decay of ^{12}C resonances. An extensive discussion of why this gives relatively good descriptions of the measured distributions of several ^{12}C resonances has been provided in [82]. The main point is that to a large extent the final state distributions are constrained by conservation laws and symmetry requirements.

The use of the $\alpha - \alpha$ correlations from the break-up of ^{12}C resonances as a method to determine the size of the resonances similarly to what is done in high energy heavy ion collisions, and in astronomy using interferometry techniques has been explored [83], but no clear sensitivity was found. Kokalova et $al.$ [84, 85] has studied emission of ^{12}C in the Hoyle-state and ^{8}Be in its ground state from the compound nucleus ^{52}Fe and suggests that enhanced emission of these states over statistical emission of two or three α-particles can be expected due to the large spatial extension of these states, which leads to a reduced Coulomb barrier for the emission. In a similar way, the sequential decay channel ^{12}C$\rightarrow \alpha + ^8$Be could be evidence for α-condensed cluster structure of the Hoyle-state and of ^{8}Be. This is in contrast to the conjectures in [76], where the condensate nature of the wave-function was believed to be evidenced by a direct decay channel.

21

5.3 *Electromagnetic probes*

Jenkins has recently provided a more general review of electromagnetic transitions as a probe of nuclear clustering [105]. There are several routes to follow to specifically probe the structure of the Hoyle-state with the electromagnetic interaction; including the electromagnetic partial decay widths, population of the state in γ-transitions from above, and by using inelastic electron scattering.

From the widths and branching ratios given in Table 1 the electromagnetic partial widths, $\Gamma(E2)$ and $\Gamma(E0)$, can be readily extracted. We give the resulting values in Table 2, together with the corresponding values for the $B(E2)$ strength and the $M(E0)$ matrix element.

The $B(E2)$ value of the Hoyle-state is usually underestimated by macroscopic cluster calculations by a factor of 2-4 while models such as AMD and FMD, which take into account the α-breaking components of the wave-function, come closer to the experimental value, see, for example, the discussion in [106, 38]. Therefore, this observable is a sensitive test of models attempting to capture both α-particle and nucleon degrees of freedom.

The E0 decay width is extracted from the charge form factor for inelastic electron scattering, which is measured with exquisite precision, see Figures 3 and Refs. 8 and [42, 71]. The nuclear structure sensitivity of the inelastic form factor is discussed in detail e.g. in Refs. [38, 42]. Mainly the large size required to understand the α-decay width of the Hoyle-state is corroborated and quantified from analysis of the form factor [42]. Also the inelastic form factor is sensitive to the size of the alpha-breaking component in the wave-function [38].

The population of the Hoyle-state in γ-transitions from individual higher lying resonances has been demonstrated. Until now this has only been possible in M1 transitions from the two 1^+ states at 12.71 MeV and 15.11 MeV [107, 108]. For the isovector M1 transition from the 15.11 MeV state the $B(M1)$-value is closely related to the B_{GT} values from the members of the same isospin triplet ^{12}N and ^{12}B, which will be discussed in detail in Section 5.4. Similar to the case of the $B(E2)$ value for the cascade decay these observables are sensitive to the α-breaking component of the wave-function, and the experimental values are well reproduced e.g. by the AMD method [38].

Finally, the Hoyle-state has been populated from higher lying continuum states in the giant resonance region in both ^{9}Be(^{3}He,γ)^{12}C and ^{11}B(p,γ)^{12}C [109, 110]. These measurements were motivated by mapping out the giant dipole resonance (GDR) built on the Hoyle-state, and comparing that to the GDR built on the ground state of ^{12}C. In the weak coupling limit it is expected that the GDR built on the Hoyle-state should be shifted up in energy by the excitation energy of the Hoyle-state. There are indications for this effect in the proton capture data, but the main effect is that the cross section for capture to the Hoyle-state is much less than that to the ground state. This has been understood as an effect of the strong α-clustering of the Hoyle-state, which makes coupling to the p+^{11}B channel weak [110]. An alternative explanation [111] could be that the large size of the Hoyle-state leads to a lowering of the dipole strength in analogy to what has been observed for Halo nuclei [112]. The latter explanation could be tested by searching for strong E1 transitions to the Hoyle-state from the excitation energy region below 20 MeV in ^{12}C.

5.4 *Weak interaction probes*

The strength of the feeding of the Hoyle-state in the weak decays of the two mirror nuclei ^{12}B and ^{12}N is a sensitive probe of the α-breaking component in the wave-function of the state, see e.g. [38]. A more in-depth discussion of measurements of the β-decays of ^{12}B and ^{12}N can be found in [113, 67].

The spin and decay properties of the Hoyle-state were first firmly established in an experiment at the Kellogg Laboratory on the β-decay of ^{12}B [5] shortly after Hoyle's original prediction of the state. This work also provided the first value for the branching ratio of 1.3(4)%. Until a decade ago this value together with a measurement by Alburger, slightly later [114], were the only measurements of
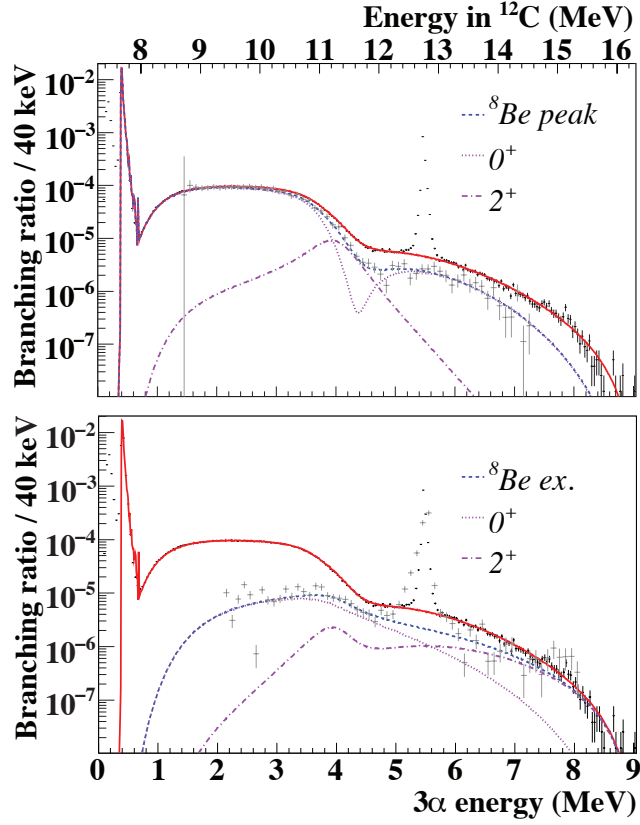
Figure 13: R-matrix fit to β-decay data for ^{12}N including three 0^+ and two 2^+ resonances (from [80]). Data from KVI, shown as black points with error bars, are shown in both plots and compared to the solid line giving the fit summed over all 3α decay channels. Data from IGISOL (grey points with error bars) for the ^{8}Be peak (top) and excited states (bottom) channels are compared to the dashed curves, which are the fit components for the respective 3α decay channels. The dotted and dot-dashed lines are contributions to each decay channel from 0^+ and 2^+ states in ^{12}C respectively.

this quantity. The branching ratio from the decay of ^{12}N was also first measured in the early 1960s in two experiments both using a Kurie-plot analysis of the positron spectrum to deduce the branching ratio [115, 116].

Due to the ghost anomaly discussed previously (Section 5.2), it is worthwhile to also keep track of information on feeding to the continuum 1-2 MeV above the Hoyle-state. Feeding to this region in the decay of ^{12}B was already identified in 1958 [117] and interpreted as a new resonance at ca. 10 MeV with spin 0^+ or 2^+. Wilkinson also found strength in this region in the decay of both ^{12}B and ^{12}N and concluded that the branching ratio was too high to only derive from the ghost anomaly, and therefore confirmed the existence of a new resonance in this region [118]. Slightly later the properties of the 10 MeV resonance were more precisely determined and the energy determined as 10.3 MeV with a large width of 3 MeV [119].

A decade ago a remeasurement of the decays of ^{12}B and ^{12}N was initiated with the aim of making use of the new techniques developed for the production and study of short-lived radioactive nuclei. A review of the results of these new experiments can be found in Ref. [67]. ^{12}B and ^{12}N have lifetimes of the order 20 ms and 10 ms respectively and the unbound states decay to three-particle final states, hence both the ISOL (isotope separation on-line) and inverse kinematics techniques are well suited to the study of these decays. For the detection of the 3α-final states, modern segmented Silicon strip detectors add the needed sensitivity over what was previously possible. Experiments at the ISOL facilities ISOLDE (CERN) [120, 121] and IGISOL (Finland) [113, 122] provided a much improved measurement of the strength 1-4 MeV above the threshold, while the Hoyle-state peak itself fell below the detection thresholds. Measurement of the feeding to the Hoyle-state peak was achieved at the KVI (the Netherlands) by producing ^{12}B and ^{12}N in inverse kinematics and implanting them in an active stopper Silicon strip detector [122] (see Fig. 13).

As a result of the remeasurements the branching ratios to the Hoyle state and the other resonances populated in the decay of ^{12}B and ^{12}N are now known with 2-3% errors rather than previously ca. 20-30% errors. Since the feeding to the Hoyle-state in both decays is reduced by a factor two over previous estimates a new measurement is under way to confirm the new low values. The idea there is to measure the E2 cascade decay populated in the β-decay of ^{12}B, i.e. product of the β-decay branching ratio and the relatively precise value for $\Gamma_{\rm rad}/\Gamma$, as an alternative route to determining the branching ratio. First results from this experiment at Argonne National laboratory using GammaSphere confirm the new low values [123]. There are plans to significantly improve the statistics of this experiment, which can lead to a new measurement of $\Gamma_{\rm rad}/\Gamma$ by using the measured value of the branching ratio from the KVI measurement.

In Refs.[121, 80] R-matrix based fits of resonances fed in the decays of ^{12}B and ^{12}N are discussed. A common result is that there is clear evidence for interference between the ghost anomaly of the Hoyle-state and higher lying 0^+ strength. There is also clear evidence for 2^+ strength, which will be discussed further in Section 6. An example of these fits is shown in Fig. 13.

It is not straight forward to define a Gamow-Teller strength for continuum structures. In practice what is most often done is to simply use the standard definition for bound states where the decay rate is $w = (\ln 2)\frac{g_A^2}{K}f(Q-E)B_{GT}$, where f is the phase space factor, $K = 2(\ln 2)\pi^3\hbar^7/(m_e^5c^4)$ (m_e being the electron mass). The beta strength B_{GT} is given by the reduced matrix element squared $|\langle f|\beta_\pm|i\rangle|^2$ and the weak interaction constant g_A is factorized out explicitly from the operator $\beta_\pm$ that flips spin and isospin. For wide resonances this becomes problematic for several reasons. One obvious problem is that the $\beta\nu$-phasespace factor f will vary over the resonance profile. The suggestion of Ref. [124] is to define the beta strength for final unbound states so that the following expression holds for the decay rate:

$$w(E){\rm d}E = \ln 2\frac{g_A^2}{K}f(Q-E)B_{GT}(E){\rm d}E \ , \tag{14}$$

This definition is in principle experimentally simple to implement, but can be more complex to use

24

theoretically since it does not depend on an interpretation of the continuum in terms of resonances or non-resonant structure. A similar caution should be observed for how to treat electromagnetic transitions in the continuum. It would clearly be desirable to have a genuine continuum calculation of the weak and electromagnetic decay into the Hoyle-state, but this is not yet available.

For the Hoyle-state the recommendation now is to not include the contribution from the ghost anomaly in the calculation of the B_{GT} strength since the region of the continuum 1-3 MeV above the threshold has more contributions than the ghost anomaly as already concluded by Wilkinson [118]. In Table 2 we give our recommended values determined in this way. Again, the methods currently best capable of reproducing these quantities are AMD and FMD, e.g. Ref. [38].

5.5 *Nuclear reaction probes*

Population of the Hoyle-state has been observed in a vast range of reaction with nuclear beams including inelatic scattering, transfer reactions, and fusion evaporation reactions.

Results from inelastic scattering reactions using stable beams from the neutron up to at least calcium are summarised in [125]. Here we will focus on the information obtained for light beams, and relatively recent experiments. Most of these measurements and analyses are motivated by the concept of "α-condensed" states. Scattering experiments have also been essential in establishing the existence of low-lying 2^+ resonances in ^{12}C, which we discuss in detail in Section 6.

High precision α-scattering data have been obtained at 240 MeV [126] and 386 MeV [127] and ^{6}Li scattering at 156 MeV [128]. These measurements all determine the isoscalar monopole strength to the Hoyle-state in the range 7-10 % of the energy weighted sum rule (EWSR), whereas theoretical estimates predict 2-3 times this quantity, and the monopole strength determined from electron scattering amounts to 15 % of the EWSR. This deficiency has been suggested to be caused by enhanced absorption in the $\alpha + ^{12}$C$^*(0_2^+)$ exit channel [129].

Ohkubo and Hirabayashi analysed the oscillation pattern of the angular distribution of ^{3}He and α inelastic scattering populating the Hoyle state, and found that the shifts of the minimal points can be used to estimate the nuclear radius of this state [130]. This has, however, been questioned by Takashina and Sakuragi who found that the minima in the angular distribution determine rather the extension of the transition density, but that the nuclear radius can be deduced from the absolute value of the differential cross section [131]. Okamoto *et al.* has performed a high precision proton scattering experiment at 200 MeV and analysed the transition densities for three types of cluster-models and find that microscopic cluster models describe the data well [132].

Danilov *et al.* analysed inelastic scattering in a diffraction model and determined the radius of the Hoyle-state to be 20 % larger than the ground state [133]. Belyaeva *et al.* analysed large angle inelastic α-scattering and demonstrate a sensitivity to the relative angular momentum between the α-particles in the Hoyle-state [134]. Finally, Hamada *et al.* analyse the Airy minimum of the pre-rainbow scattering of 50-60 MeV ^{3}He off ^{12}C and deduce at large extension of the Hoyle-state [135].

We next turn to transfer reactions. [125] list an extensive set of reactions populating the Hoyle-state including ^{9}Be$(\alpha,$n$)^{12}$C, ^{10}B$(^3$He,p$)^{12}$C, ^{11}B$(^3$He,d$)^{12}$C, ^{13}C(p, d)^{12}C, ^{14}N(d,$\alpha)^{12}$C and ^{15}N(p,$\alpha)^{12}$C. Transfer reactions have for many years been a standard tool to analyse the nuclear structure of isolated states through optical potentials, extraction of spectroscopic factors and comparison to Shell-model predictions. At first sight it is therefore somewhat surprising that there has been very little work done on the structure of the Hoyle-state from this method. In most studies where population of the Hoyle-state is seen, this data is simply bypassed and the attention focused on other states. In most transfer reactions the Hoyle-state is weakly populated, which is also what one would expect because formation of a strongly clustered state should be difficult in e.g. stripping and pickup reactions from p-shell nuclei. On the other hand, the fact that the Hoyle-state is populated in these reactions means that there must be a sizeable p-shell component in the wave-function. As already discussed, this conclusion

25

Table 2: Selected range of properties of the Hoyle-state

Property	Adopted value	Comments
Energy	7.65407(19) MeV	Average from [68]
Total width	9.3(9) eV	Deduced from table 1
Dimensional reduced width	1.5	Assuming R=6 fm
Γ_{E2}	3.7(4) meV	Deduced from table 1
B(E2)	2.7(3) $e^2 fm^4$.	
	8.1(8) W.u.	
Γ_{E0}	62(2) μeV	From table 1
$M(E0)$	5.47(9) fm^2	from [71]
$B_{GT}(^{12}N)$	0.090(2)	Peak value
$B_{GT}(^{12}B)$	0.108(3)	Peak value
B(M1)(1$^+$, T=1)	1.5(2) eV	Average of [107, 108]
	0.32(5) $\mu_N{}^2$	
	0.18(3) W.u.	
B(M1)(1$^+$, T=0)	0.5(3) eV	from [107]
	0.3(2) $\mu_N{}^2$	
	0.18(11) W.u.	

is corroborated by analysis of the B_{GT} strength, M1 population, and the strength of the E2 cascade decay.

5.6 Summary

In table 2 we have collected some of the experimental quantities discussed in the text.

From the α-decay rate it is clear that the size of the Hoyle-state is large, and that the degree of clustering is high. The large size is supported by inelastic scattering reactions using both electrons and nuclear probes. The nature of the α-cluster component of the state is probed by the final state distribution of the α-decay, which points to a dominating $\alpha+^8$Be(0$^+$) structure. To some extent this is supported by analysis of the large angle inelastic scattering cross section. Evidence for p-shell components in the wave function comes from the β-decay studies and from electromagnetic population and decay of the state.

6 Hoyle-state band?

As already discussed, as early as 1956 it was suggested that the Hoyle state could be highly deformed [29]. However, experimental verification of this conjecture has been slow to materialise. For a long time, it was believed [136] that a broad structure seen in the β-decay of ^{12}B [117] was the first rotational (2$^+$)
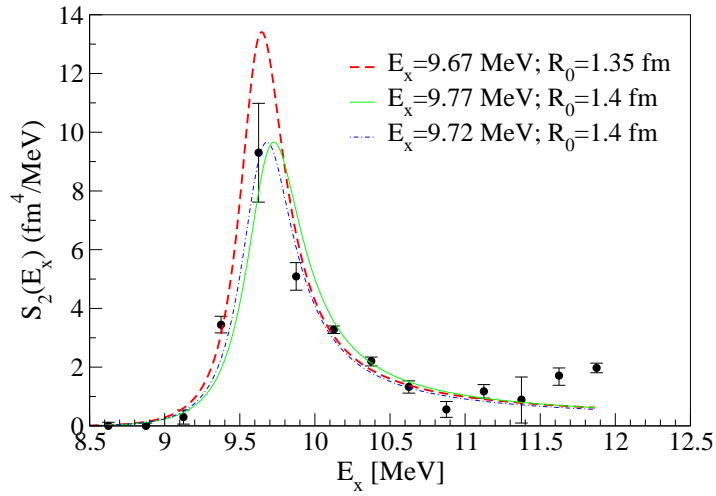
Figure 14: The spin 2 strength function ($S_2(Ex)$) extracted from the multipole decomposition analysis [127] (data points) compared with the R-matrix line-shapes associated with different channel radii and excitation energies. [140].
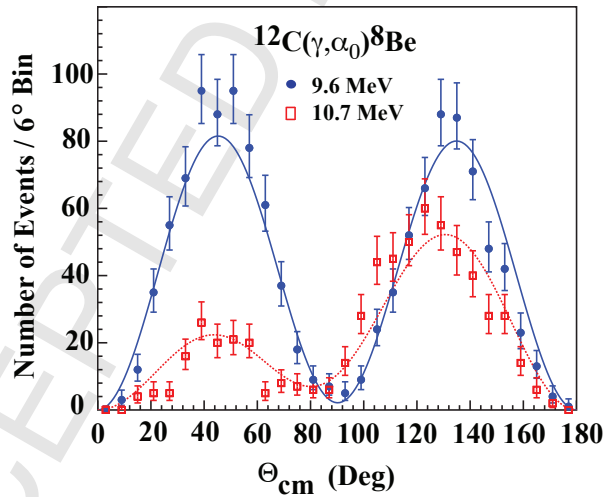

Figure 15: Angular distribution for $^{12}C(\gamma,\alpha_0)^8Be$ events measured at a beam energy of 9.6 and 10.7 MeV. The solid curve is the fit that included E1 and E2 amplitudes [144].
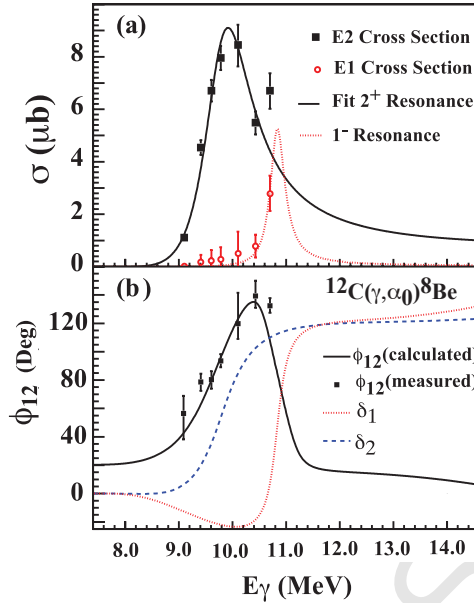
27

Figure 16: (a) The measured E1 and E2 cross sections of the ^{12}C(γ,α_0)^{8}Be reaction. (b) The measured E1-E2 relative phase angle (ϕ_{12}) together with the phase angle calculated from a two-resonance model [144].

excitation of the Hoyle-state. However, in 2005 the β-decays of both ^{12}B and ^{12}N were used to show that this structure is dominated by a broad 0^+ resonance [120] as discussed in Section 5.4 (Fig. 13). This conclusion is consistent with the results of inelastic scattering experiments [137, 138, 127]. However, these experiments also find evidence for a 2^+ resonance in the same energy region as the broad 0^+ resonance. A common analysis of the evidence for a 2^+ resonance from the proton- and α-particle scattering data is given in [140], and a discussion of the impact of these measurements is given in [139]. The 2^+ lineshape which is found in the inelastic scattering measurements ^{12}C(α,α') and ^{12}C(p,p') [140] is shown in Fig. 14. The energy of the 2^+ resonance is here determined as $E_x = 9.75(0.15)$ MeV with a width of 750(150) keV.

In the latest analysis of the β-decay data [80], there are also indications for the existence of 2^+ resonances, but the lowest one is about an MeV above the resonance found in the scattering experiments (Fig. 13). A search for a resonance at that energy in the ^{11}B(^{3}He,d)^{12}C reaction was unsuccessful [141]. The feebleness of the population of the 2^+ resonance in the α-scattering experiments [126, 127] has been analysed in detail by Cong Cuang, Khoa and Kanada-En'yo [142, 143] and explained to be mainly an effect of the overlapping 3^- and 0^+ resonances.

The existence of the 2^+ resonance seen in the proton- and α-particle scattering experiments was recently confirmed by a measurement of the ^{12}C(γ,3α) reaction at the HIγS facility [144]. The angular distributions of the emitted α-particles are shown in Fig. 15 at two different beam energies; 9.6 and 10.7 MeV. These reveal both an E2 term plus an interference with an E1 component. The E2 component is associated with the newly discovered 2^+ resonance and the E1 the known 1^- state at 10.8 MeV. Fig. 16 shows the 2^+ line shape and the phase angle extracted from the data compared with that calculated from the interference of the two resonances

$$\phi_{12} = \delta_2 - \delta_1 + \tan^{-1}(\eta/2) \tag{15}$$

where the nuclear phase shifts δ are given by the resonance phase shift minus the hard sphere phase shift and η is the Sommerfeld parameter [144].

28

In addition, this experiment provides a value for the electromagnetic transition rate between the ground state and the 2^+ resonance, which can be used to test models of its structure, and is important for assessing the influence of this new resonance on the 3α reaction rate. The value given in [144] has been corrected to 0.96(8) W.u. due to an error in the R-matrix formula [145]. The energy and width of the 2^+ resonance determined by this experiment is $E_x = 10.13(6)$ MeV and $\Gamma = 2.1(3)$ MeV [145], which indicates a somewhat wider resonance compared to what is determined from the scattering experiments [140].

Evidence is also emerging for the existence of a 4^+ resonance in the neighbourhood of the well-known 4^+ resonance at 14.2 MeV [146]. This is supported by a preliminary report [147]. It is somewhat surprising that there is no effect of interference between the two 4^+ resonances such as asymmetric line-shapes. Such effects would be interesting to search for. Finally, there is first evidence for a resonance with even higher spin from the Birmingham group [148, 149], with an indication of a 5^- state at $\sim$22.4 MeV.

It is obviously of great interest to understand how these new resonances may form rotational bands. It is not clear at present which 0^+ resonance may be linked to the new 2^+ and 4^+ resonances as a band head. From calculated electromagnetic transitions rates [38, 142, 143] it appears that the third 0^+ state has by far the highest transition rate to the 2^+ resonance and therefore it may be more connected to the new resonances than the Hoyle-state. A natural conjecture would be that more 2^+ resonances exist in the same energy region to match the number of 0^+ resonances. The elucidation of this will be a major and challenging task for the future. It may also be that the concept of a rotational band is inadequate for resonances as broad as found in ^{12}C. The interpretation of the 0^+, 2^+, 4^+ band in ^{8}Be has recently been challenged by a calculation of the transition rates between those resonances including non resonant contributions [150]. This calculation indicates that the naive picture of a common intrinsic structure in that band is invalid and the intrinsic structure for the 0^+, 2^+, 4^+ resonances quite different. A similar conclusion emerges for the Hoyle-band from the AMD calculations [38].

7 Outlook and future work

From an experimental perspective the nature of the spectroscopy above the ^{12}C α-decay threshold has been advanced significantly, with the existence of a 2^+ resonance approximately 2 MeV above the Hoyle-state being firmly established. The character of the state and its relationship to the Hoyle-state has yet to be understood, though there are strong indications from its electromagnetic properties and deduced reduced α-decay width that it too possesses a well-developed α-cluster structure. It is possible that there is further 2^+ strength at higher excitation energies which remains to be fully characterised. Moreover, the nature of the 0_3^+ state and its relationship to the 2^+ state is yet to be understood. There are indications of a broad 4^+ excitation at 13.3 MeV, but further work is required to demonstrate its existence unambiguously. Arriving at a detailed understanding of the spectroscopy of ^{12}C in this region is challenging due to the broad widths of the states and the fact that there are a number of competing structures associated with both the 0_2^+ and 0_3^+ states. What is required are high statistics precision measurements using a range of probes which include electromagnetic, weak and strong interactions. As a starting point, detailed measurements of the α-decay correlations following proton and α-inelastic scattering measurements utilising the energy resolution which may be achieved with a spectrometer, but harnessing the selectivity associated with the decay channel selection would be an advance as, for example, demonstrated for ^{12}C resonances in the 16-24 MeV range in a proton scattering experiment at 156 MeV [151].

The second 2^+ state has yet to be observed in the β-decay measurements. At present this is taken as an indication of the small overlap of the parent states in ^{12}N and ^{12}B and hence the well-developed cluster structure. A definitive measurement of the 2^+ state in this weak channel is important in providing a

29

detailed understanding of the degree to which clustering is developed in the 2^+ state. Given the β-decay demonstrably feeds the Hoyle-state it is likely that the degree of clusterisation in the 2^+_2 state is larger than that encountered in the Hoyle-state.

Ultimately, measurements of the electromagnetic transition strengths, $B(E2)$, between the states above the α-decay threshold are the litmus test of which states may be strongly structurally linked. Such measurements have been performed for ^{8}Be between the 2α 4^+ and 2^+ cluster states [152]. In that instance the states are separated by close to 8 MeV and hence the transition probability is strongly amplified by the E^5 dependence of the $B(E2)$ reduced transition amplitude. Hence, the competition with the α-decay is enhanced and a measurement is possible. In the case of the transition between the states in ^{12}C which have been linked to the Hoyle-band, the electromagnetic decay rate is likely to be further reduced by up to a factor of 10^3. Such a measurement would truly be a tour de force.

For the Hoyle-state itself, precision measurements of the radiative widths and the direct, non-sequential, 3α decay branches are important for both the astrophysical and structural implications and it is likely that improved numbers will appear shortly. It is also feasible to measure the population of the Hoyle-state in E1 transitions from resonances below the GDR region and thereby explore if the missing strength at higher energy has moved down in energy due to the large spatial extension of the Hoyle-state.

It is likely that as state-of-the-art, ab initio, theory further develops that ^{12}C will continue to be a key testing ground as it displays the almost unique element of a transition from a ground state strongly allied to the shell-model limit to an excited state which demonstrates one of the most strongly developed cluster structures known. Understanding this transition underpins a deeper knowledge of nucleon-nucleon correlations and many-body effects in nuclei per se. Inclusion of continuum effects in the ab-initio calculations will be an essential goal in order to fulfil this programme.

References

[1] E. Öpik, *Proceedings of the Royal Irish Academy* A 54 (1951) 49

[2] E.E. Salpeter *Astrophysical Journal* 115 (1952) 326

[3] F. Hoyle *Astrophysical Journal, Supplement Series* 1 (1954) 12

[4] D.N.F. Dunbar, R.E. Pixley, W.A. Wenzel and W. Whaling *Phys. Rev.* 92 (1953) 649

[5] C.W. Cook, W.A. Fowler, C.C. Lauritsen and T. Lane *Phys. Rev.* 107 (1957) 508

[6] J.D. Barrow and F.J. Tipler *The Anthropic Cosmological Principle* Cambridge University Press, 1986

[7] B. Carter *Confrontation of Cosmological Theories with Observational Data* Dordecht: Reidel (1974) 291

[8] H. Kragh *Archive for History of Exact Sciences* 64 (2010) 721

[9] M.G. Holloway and B.L. Moore *Phys. Rev.* 58 (1940) 847

[10] R. Malm and W. W. Buechner *Phys. Rev.* 81 (1951) 519

[11] L. R. Hafstad, E. Teller, *Phys. Rev.* 54 (1938) 681

[12] K. Ikeda, *et al.*, Prog. Theor. Phys. Suppl., Extra Numbers (1968) 464

[13] E. Epelbaum, H. Krebs, T.A. Lähde, D. Lee, and Ulf-G. Meißner *Phys. Rev. Lett.* 110 (2013) 112502

[14] Y. Funaki, H. Horiuchi, W. von Oertzen, G. Roepke, Peter Schuck, A. Tohsaki, T. Yamada *Phys. Rev.* C 80 (2009) 064326

[15] Cauldrons in the Cosmos: Nuclear Astrophysics. Rolfs, Claus E.;Rodney, William S. Published by Chicago, Illinois, U.S.A.: Univ of Chicago Pr, 1988

[16] H. Bethe *Phys. Rev.* 55 (1939) 434

[17] Karlsruhe Gamow window calculator: http://www.kadonis.org/pprocess/gamow.php

[18] K. Ogata, M. Kan, M. Kamimura, *Prog. Theor. Phys.* 122 (2009) 1055

[19] N. B. Nguyen, F. M. Nunes, I. J. Thompson, E. F. Brown, *Phys. Rev. Lett.* 109 (2012) 141101 ; N. B. Nguyen,F. M. Nunes, and I. J. Thompson, *Phys. Rev. C* 87 (2013) 054615

[20] E. Garrido, R. de Diego, D.V. Fedorov, and A.S. Jensen, *Eur. Phys. J. A* 47 (2011) 102

[21] S. Ishikawa, *Phys. Rev. C* 87 (2013) 055804

[22] K. Yabana and Y. Funaki *Phys. Rev. C* 85 (2012) 055803 ; T. Akahori, Y. Funaki, K. Yabana, arXiv:1401.4390 [nucl-th]

[23] S.M. Austin, C. West, and A. Heger, *Phys. Rev. Lett.* 112 (2014) 111101

[24] S. Karataglidis, *et al. Phys. Rev. C* 52 (1995) 861

[25] H. Marenau *Phys. Rev. C* 59 (1941) 37

[26] D.M. Brink *Proceedings of the International School of Physics "Enrico Fermi"*, Varenna, 1965, Course 36, edited by C. Bloch (Academic Press, New York 1966), p. 247

[27] D.M. Brink *Nucl. Phys. A* 91 (1967) 1

[28] D.M. Brink *Journal of Physics: Conference Series* 111 (2008) 012001

[29] H. Morinaga, *Phys. Rev.* 101 (1956) 254

[30] I. Sick and J.S. McCarthy, *Nucl. Phys. A* 150 (1970) 631 ; A. Nakada, Y. Torizuka and Y. Horikawa, *Phys. Rev. Lett.* 27 (1971) 745 ; and 1102 (Erratum); P. Strehl and Th. H. Schucan, *Phys. Lett. B* 27 (1968) 641

[31] Y. Funaki, *et al.*, *Eur. Phys. J. A* 28 (2006) 259

[32] A. Tohsaki, *et al.*, *Phys. Rev. Lett.* 87 (2001) 192501

[33] Y. Funaki, A. Tohsaki, H. Horiuchi, P. Schuck and G. Röpke, *Phys. Rev. C* 67 (2003) 051306

[34] T. Yamada and P. Schuck, *Phys. Rev. C* 69 (2004) 024309

[35] T. Yamada and P. Schuck, *Eur. Phys. J. A* 26 (2005) 185

[36] Y. Funaki *et al.*, *Eur. Phys. J. A* 24 (2005) 321

[37] Y. Kanada En'yo and H. Horriuchi *Prog. Theor. Phys.* 142 (2001) 205

[38] Y. Kanada En'yo *Prog. Theor. Phys.* 117 (2007) 655

[39] T. Marumori, J. Phys. Soc. Jpn. 44 (1978), 225. M. Kamimura, Nucl. Phys. A 351 (1981), 456.

[40] E. Uegaki, S. Okabe, Y. Abe and H. Tanaka, Prog. Theor. Phys. 57 (1977), 1262. E. Uegaki, Y. Abe, S. Okabe and H. Tanaka, *Prog. Theor. Phys.* 59 (1978) 1031 ; *Prog. Theor. Phys.* 62 (1979) 1621

[41] R. Roth, T. Neff, H. Feldmeier, Prog. Part. Nucl. Phys. 65 (2010) 50

[42] M. Chernykh, *et al.*, *Phys. Rev. Lett.* 98 (2007) 032501

[43] J. Fujita and H. Miyazawa, *Prog. Theor. Phys.* 17 (1957) 360

[44] R. B. Wiringa, Steven C. Pieper, J. Carlson, and V. R. Pandharipande, *Phys. Rev. C* 62 (2000) 014001

[45] S. C. Pieper, K. Varga, and R. B. Wiringa *Phys. Rev. C* 66 (2002) 044310

[46] R. B. Wiringa and S. C. Pieper, *Phys. Rev. Lett.* 89 (2002) 182501

[47] V. Bernard and U-G. Meißner, Ann. Rev. of Nucl. Part. Sci. **57**, 33 (2007).

[48] P. Navrátil, S. Quaglioni, I. Stetcu and B. R. Barrett J. Phys. G **36**, 083101 (2009).

[49] P. Navrátil, *et al.*, Phys. Rev. Lett. **84**, 5728 (2000).

[50] P. Maris, J. P. Vary and P. Navrátil, Phys. Rev. C **87**, 014327 (2013).

[51] M Freer, *Rep. Prog. Phys.* 70 (2012) 2149

[52] A.C. Dreyfuss *et al. Phys. Lett.* B 727 (2013) 511

[53] E. Epelbaum, *et al. Phys. Rev. Lett.* 109 (2012) 252501

[54] E. Epelbaum, *et al. Phys. Rev. Lett.* 106 (2011) 192501

[55] R. Bijker, F. Iachello, and A. Leviatan, *Ann. Phys.* 236 69 (1994)

[56] R. Bijker, A.E.L. Dieperink, and A. Leviatan; *Phys. Rev. A* 52 2786 (1995)

[57] R. Bijker and F. Iachello, *Phys. Rev.* C 61 (2000) 067305

[58] M. Freer *et al.*, *Phys. Rev.* C 76 (2007) 034320

[59] O.S. Kirsebom *et al. Phys. Rev.* C 81 (2010) 064313

[60] J. Okołowicz, W. Nazarewicz and M. Płoszajczak *Fortschritte der Physik* 61 (2013) 66

[61] M. Freer, *Nature* 487 (2012) 309

[62] J.-P. Ebran, E. Khan, T. Niksic and D. Vretenar *Nature* 487 (2012) 341

[63] P. Papka and C. Beck, chap.6 in *Clusters in Nuclei*, C. Beck (ed.), *Vol 2*, Lecture Notes in Physics 848, DOI: 10.1007/978-3-642-24707-1_6, Springer-Verlag, Berlin Heidelberg 2012.

[64] L.R. Buchmann and C.A. Barnes, *Nucl. Phys.* A 777 (2006) 254

[65] T. Kibedi, A.E. Stuchbery, G.D. Dracoulis and K.A. Robertson, EPJ Web of Conferences 35, 06001 (2012)

[66] B. Alshahrani *et al.* EPJ Web of Conferences 63, 01022 (2013)

[67] H.O.U. Fynbo and C. Aa. Diget, Hyperfine Interactions, 223, 103 (2014)

[68] J.A. Nolen, and S.M. Austin, *Phys. Rev.* C 13 (1976) 1773

[69] C. Tur *et al.*, Nucl. Inst. Meth., A594, 66 (2008).

[70] H. Crannell *et al. Nucl. Phys.* A 758 (2005) 399c

[71] M. Chernykh *et al.*, *Phys. Rev. Lett.* 105 (2010) 022501

[72] A. M. Mukhamedzhanov and A. S. Kadyrov *Phys. Rev.* C 82 (2010) 051601

[73] C. Illiadis, *Nucl. Phys.* A 618 (1997) 166

[74] F.C. Barker and P.B. Treacy, *Nucl. Phys.* 38 (1962) 33

[75] M. Freer *et al.*, *Phys. Rev.* C 49 (1994) R1751

[76] Ad. R. Raduta *et al.*, *Phys. Lett.* B 705 (2011) 65

[77] O.S. Kirsebom *et al.*, *Phys. Rev. Lett.* 108 (2012) 202501

[78] J. Manfredi *et al.*, *Phys. Rev.* C 85 (2012) 037603

[79] T.K. Rana *et al.*, *Phys. Rev.* C 88 (2013) 021601(R)

[80] S. Hyldegaard *et al. Phys. Rev.* C 81 (2010) 024303

[81] R. Alvarez-Rodriguez *et al.*, *Phys. Rev. Lett.* 99 (2007) 072503

[82] H.O.U. Fynbo *et al.*, *Phys. Rev.* C 79 (2009) 054009

[83] M. Freer, J. Phys. G: Nucl. Part. Phys. 34 789 (2007)

[84] Tz. Kokalova *et al.*, *Eur. Phys. J.* A 23 (2005) 19

[85] Tz. Kokalova, N. Itagaki, W. von Oertzen, and C. Wheldon, *Phys. Rev. Lett.* 96 (2006) 192502

[86] D.E. Alburger, *Phys. Rev.* C 124 (1961) 193

[87] P.A. Seeger, R.W. Kawanash, Astrophys. J. 137 (1963) 704, *Nucl. Phys.* 46 (1963) 577

[88] I. Hall and N.W. Tanner, *Nucl. Phys.* 53 (1964) 673

[89] D. Chamberlin *et al.*, *Phys. Rev.* C 9 (1974) 69

[90] C.N. Davids *et al.*, *Phys. Rev.* C 11 (1975) 2063

[91] H.B. Mak, et al., *Phys. Rev.* C 12 (1975) 1158

[92] R.G. Markham, S.M. Austin, and M.A.M. Shahabuddin, *Nucl. Phys.* A 270 (1976) 489

[93] A.W. Obst and W.J. Braithwaite, *Phys. Rev.* C 13 (1976) 2033

[94] D.E. Alburger, *Phys. Rev.* 118 (1960) 235

[95] F. Ajzenberg-Selove and P.H. Stelson, *Phys. Rev.* 120 (1960) 500

[96] A.W. Obst *et al.*, *Phys. Rev.* C 5 (1972) 738

[97] R.G.H. Robertson *et al.*, *Phys. Rev.* C 15 (1977) 1072

[98] D.E. Alburger, PRC 16 (1977) 2394

[99] J.H. Fregau, *Phys. Rev.* 104 (1956) 225

[100] H.L. Crannell and T.A. Griffy, *Phys. Rev.* 136 (1964) B1580

[101] F. Gudden and P. Strehl, *Z. Phys.* A 185 (1965) 111

[102] H. Crannell *et al.*, *Nucl. Phys.* A 90 (1967) 152

[103] P. Strehl and T.H. Schucan, *Phys. Lett.* B 27 (1968) 641

[104] P. Strehl, *Z. Phys.* 234 (1970) 416

[105] D. Jenkins, chap.2 in *Clusters in Nuclei*, C. Beck (ed.), *Vol 3*, Lecture Notes in Physics 875, DOI: 10.1007/978-3-319-01077-9_2, Springer-Verlag, Berlin Heidelberg 2012.

[106] N. Itagaki, S. Aoyama, S. Okabe and K. Ikeda, *Phys. Rev.* C 70 (2004) 054307

[107] O.S. Kirsebom *et al.*, *Phys. Lett.* B 680 (2009) 44

[108] D.E. Alburger and D.H. Wilkinson, *Phys. Rev.* C 5 (1977) 384

[109] H.D. Shay *et al.*, *Phys. Rev.* C 9 (1974) 76

[110] K.A. Snover, P.Paul, and H.M. Kuan, *Nucl. Phys.* A 285 (1977) 189

[111] K. Riisager, private communication.

[112] P.G. Hansen and B. Jonsen, Europhys Lett. 4 409 (1987)

[113] S. Hyldegaard *et al.* Phys. Rev. C 80 (2009) 044304

[114] D. E. Alburger, *Phys. Rev.* 131 (1963) 1624

[115] T. Mayer-Kuckuk and F. C. Michel, *Phys. Rev.* 127 (1962) 545

[116] R. W. Peterson and N. W. Glass, *Phys. Rev.* 130 (1963) 292

[117] C. W. Cook, W. A. Fowler, C. C. Lauritsen and T. Lauritsen, *Phys. Rev.* 111 (1958) 567

[118] D. H. Wilkinson, D. E. Alburger, A. Gallmann and P. F. Donovan, *Phys. Rev.* 130 (1963) 1953

[119] D. Schwalm and B. Povh, *Nucl. Phys.* 89 (1966) 401

[120] H.O.U. Fynbo *et al.*, *Nature* 433 (2005) 136

[121] C. Aa. Diget *et al.*, *Nucl. Phys.* A 760 (2005) 3

[122] S. Hyldegaard *et al.* Phys. Lett. B 678 (2009) 459

[123] M. Alcorta *et al.*, EPJ Web of Conferences 66, 07001 (2014)

[124] K. Riisager, *Nucl. Phys.* A 925 (2014) 112

[125] F. Ajzenberg-Selove, *Nucl. Phys.* A 506 (1990) 1

[126] B. John *et al.*, *Phys. Rev.* C 68 (2003) 014305

[127] M. Itoh *et al.*, *Phys. Rev.* C 84 (2011) 054308

[128] W. Eyrich *et al.*,*Phys. Rev.* C 36 (1987) 416

[129] D.T. Khoa and D. Cong Cuong, *Phys. Lett.* B 660 (2008) 331

[130] S. Ohkubo1 and Y. Hirabayashi, *Phys. Rev.* C 70 (2004) 01602(R)

[131] M. Takashina and Y. Sakuragi, *Phys. Rev.* C 74 (2006) 054606

[132] A. Okamoto *et al.*, *Phys. Rev.* C 81 (2010) 054604

[133] A. N. Danilov, T. L. Belyaeva, A. S. Demyanova, S. A. Goncharov, and A. A Ogloblin, *Phys. Rev.* C 80 (2009) 054603

[134] T. L. Belyaeva *et al.*, *Phys. Rev.* C 82 (2010) 054618

[135] Sh. Hamada, Y. Hirabayashi, N. Burtebayev, and S. Ohkubo *Phys. Rev.* C 87 (2013) 024311

[136] H. Morinaga, Phys. Lett. **21**, 78 (1966)

[137] M. Freer *et al.*, *Phys. Rev.* C 80 (2009) 041303

[138] W. R. Zimmerman *et al.*, *Phys. Rev.* C 84 (2011) 027304

[139] H.O.U. Fynbo and M. Freer, Physics, 4, 94 (2011)

[140] M. Freer *et al.*, *Phys. Rev.* C 86 (2012) 034320

[141] M.D. Smit *et al.* *Phys. Rev.* C 86 (2012) 037301

[142] D.T. Khoa, D.C. Cuong, and Y. Kanada-Enyo, *Phys. Lett.* B 695 (2011) 469

[143] D.C. Cuong, D.T. Khoa, and Y. Kanada-Enyo, *Phys. Rev.* C 88 (2013) 064317

[144] W.R. Zimmerman *et al.*, *Phys. Rev. Lett.* 110 (2013) 152502

[145] W.R. Zimmerman, PhD thesis, and private communication.

[146] M. Freer *et al.*, *Phys. Rev.* C 83 (2011) 034314

[147] Jyvaskyla accelerator news, vol 21, March 2013; Ogloblin *et al.* EPJ Web of Conferences 66, 02074 (2014)

[148] Tz. Kokalova EPJ Web of Conferences 66 03046 (2014)

[149] Accepted for publication in *Phys. Rev. Lett.* ()

[150] E. Garrido, A.S. Jensen, D.V. Fedorov, *Phys. Rev.* C 88 (2013) 024001

[151] J.A. Templon *et al.*, *Phys. Lett.* B 413 (1997) 253

[152] V. M. Datar, *et al.*, *Phys. Rev. Lett.* 111 (2013) 062502